2016

Defining the Role of a Putative Peptidase in Staphylococcus Aureus Quorum Sensing and Pathogenesis

Chelsea Rose White
Loyola University Chicago

LOYOLA UNIVERSITY CHICAGO

DEFINING THE ROLE OF A PUTATIVE PEPTIDASE IN *STAPHYLOCCOCUS AUREUS* QUORUM SENSING AND PATHOGENESIS

A THESIS SUBMITTED TO

THE FACULTY OF THE GRADUATE SCHOOL

IN CANDIDACY FOR THE DEGREE OF

MASTER OF SCIENCE

PROGRAM IN INFECTIOUS DISEASE AND IMMUNOLOGY

BY

CHELSEA ROSE WHITE

CHICAGO, ILLINOIS

AUGUST 2016

ACKNOWLEDGEMENTS

I would like to thank everyone who has supported me during my time in graduate school. I am particularly grateful to my mentor Dr. Francis Alonzo III who was willing to take me into his laboratory and whose mentorship has been critical to me developing a zeal for bench work. I would also like to acknowledge my entire thesis committee for encouraging me and challenging me as a student and a scientist.

I would like to thank all the members of the Alonzo lab for their advice, help, and humor. Especially, James Grayczyk for the endless supply of macrophages and jokes along with Azul Zorzoli for reminding me there is so much more ahead of us. An immense amount of gratitude goes to my parents for sacrificing so much for me and my education, while inspiring me, teaching me, and loving me. Matt, thank you for reading these pages more then you probably cared to and for keeping me caffeinated through the thick and thin of this process. It truly took a village to get me here and I thank you all.

TABLE OF CONTENTS

LIST OF TABLES

LIST OF FIGURES

ABSTRACT

The pathogenic bacterium *Staphylococcus aureus* encounters a variety of immune cells that restrict bacterial growth and dissemination during infection. However, *S. aureus* counters these immune cell functions by producing myriad virulence factors that facilitate evasion of host defense strategies. Therefore, it is important to understand *S. aureus*-immune cell interactions and the virulence factors that perturb normal immune function to promote pathogenesis. In a genetic screen designed to identify *S. aureus* secreted factors that positively or negatively modulate macrophage activity our lab identified a transposon insertion mutant in the gene *SAUSA300_1984*, encoding a putative membrane spanning peptidase. To investigate the role of 1984 in pathogenesis, I generated a Δ*1984* mutant and found it behaves like a quorum sensing system mutant, Δ*agr*, with defects in protein secretion and macrophage activation. The Agr system requires proper processing of a signaling peptide, AgrD, via cleavage of its C-terminus by AgrB and cleavage of its N-terminus by an unknown peptidase. Given this information, I hypothesized that 1984 is a peptidase is involved in processing AgrD.

If 1984 is involved in AgrD processing, then loss of its activity will perturb virulence factor production, enhance immune cell activity, and attenuate virulence. Thus, this study aimed to determine how this membrane-spanning putative peptidase elicits global changes in virulence factor gene expression, via the Agr system, with subsequent influences on macrophage activation and pathogenesis.

CHAPTER ONE

LITERATURE REVIEW

Staphylococcus aureus **can lead to severe infections.**

Staphylococcus aureus is a major cause of infectious conditions such as sepsis, endocarditis, toxic shock syndrome, and bacteremia. Both hospital-acquired and community-acquired *S. aureus* infections have increased in recent decades leading to a 62% increase in hospitalizations from 1999 to 2005 (1) and thousands of deaths per year (2, 3). Part of this increase is attributed to the increased incidence of antibiotic resistance among infectious isolates as evidenced by a doubling in the number of methicillin-resistant *S. aureus* (MRSA)-related hospitalizations over a six-year period (1). Despite being a major cause of these serious illnesses, *S. aureus* is also a common transient commensal and colonizes up to 50 percent of healthy adults (4). Typically, infections occur when *S. aureus* breaches the skin or mucosal barriers. Upon entry into a sterile site, *S. aureus* encounters a rapid pro-inflammatory innate immune response that poses a significant obstacle to bacterial dissemination. The interactions between *S. aureus* and some of these immune cells, such as neutrophils, are very well studied (5) while other interactions, such as between *S. aureus* and macrophages, are less well understood. It is known that *S.aureus* uses complex and redundant virulence gene regulatory systems to

produce an array of cytotoxins and immunomodulatory proteins that promote evasion of immune surveillance mechanisms and promote bacterial survival during infection.

***S. aureus* virulence factor gene expression is controlled by complex regulatory systems.** The ability of *S. aureus* to colonize a wide range of tissues and cause acute and chronic disease is partially due to its use of complex regulatory systems that control the expression of a myriad virulence factors. Of these virulence factors, *S. aureus* secretes toxic proteins that can cause tissue damage and facilitate the spread of infection, as well as surface proteins that promote resistance to phagocytosis or antimicrobial peptides (6). These virulence factors are often regulated at multiple levels including translation, transcription, and degradation (7). *S. aureus* employs 16 two-component systems as a part of its regulatory network (7). Furthermore, many of these two-component regulatory systems not only directly control gene expression, but also control expression of regulatory RNAs (7). One example of a major two-component regulatory system in *S. aureus* that regulates virulence factor production as well as a regulatory RNA is the Accessory Gene Regulatory system, or Agr system.

A peptide-based quorum sensing system regulates virulence factor gene expression in *S. aureus*. The Agr system is a well-documented peptide-based quorum sensing system involved in promoting secretion of major *S aureus* virulence factors (Figure 1). All of the known components of the Agr system are transcribed from the *P2* promoter as a polycistronic mRNA with 4 open reading frames (8). Agr is comprised of AgrA, a response regulator (9), AgrB, a metalloprotease that modifies AgrD and aids in

transport of processed peptide (10-13), AgrC, a histidine kinase (14), and AgrD, the precursor of the auto-inducing peptide, AIP. Clinical isolates of *S. aureus* contain one of four distinct Agr groups, each with a sequence specific AgrD (Groups I, II, III, and IV) (15, 16). AgrD recognition is group specific and each of the four AgrD variants inhibits the activity of their respective non-cognate Agr groups (16). AgrD is a peptide composed of 46 amino acids that is post-translationally modified and processed in order to generate a functional AIP (Figure 1B). The N-terminal 18 residues form an α-helix that anchors the peptide to the cell membrane by lateral association (17). This anchoring seems to be required for processing of AgrD. Previously, it was shown that AgrB is involved in AgrD post-translational processing. AgrB is a multipass membrane protein with a catalytic dyad required for cleavage of the C-terminal end of the peptide between the methionine of the AIP and an aspartic acid (11, 12)(Figure 1B). This processing event is Agr group specific (10, 11). In addition, AgrB catalyzes the efficient and reversible cyclization of AgrD (18). This cyclization reaction leads to the formation of a thiolactone linkage between the C-terminal carbonyl and the sulfur atom present in a cysteine side chain of AIP (19). The thiolactone is required for recognition by the Histidine kinase, AgrC (20). The degradation of the C-terminal cleavage product from AgrD is a key component of AIP synthesis, as its degradation is predicted to provide the energy required for the thiolactone formation (18). Additionally, AgrB is hypothesized to have a direct role in secretion of the processed AIP (13).

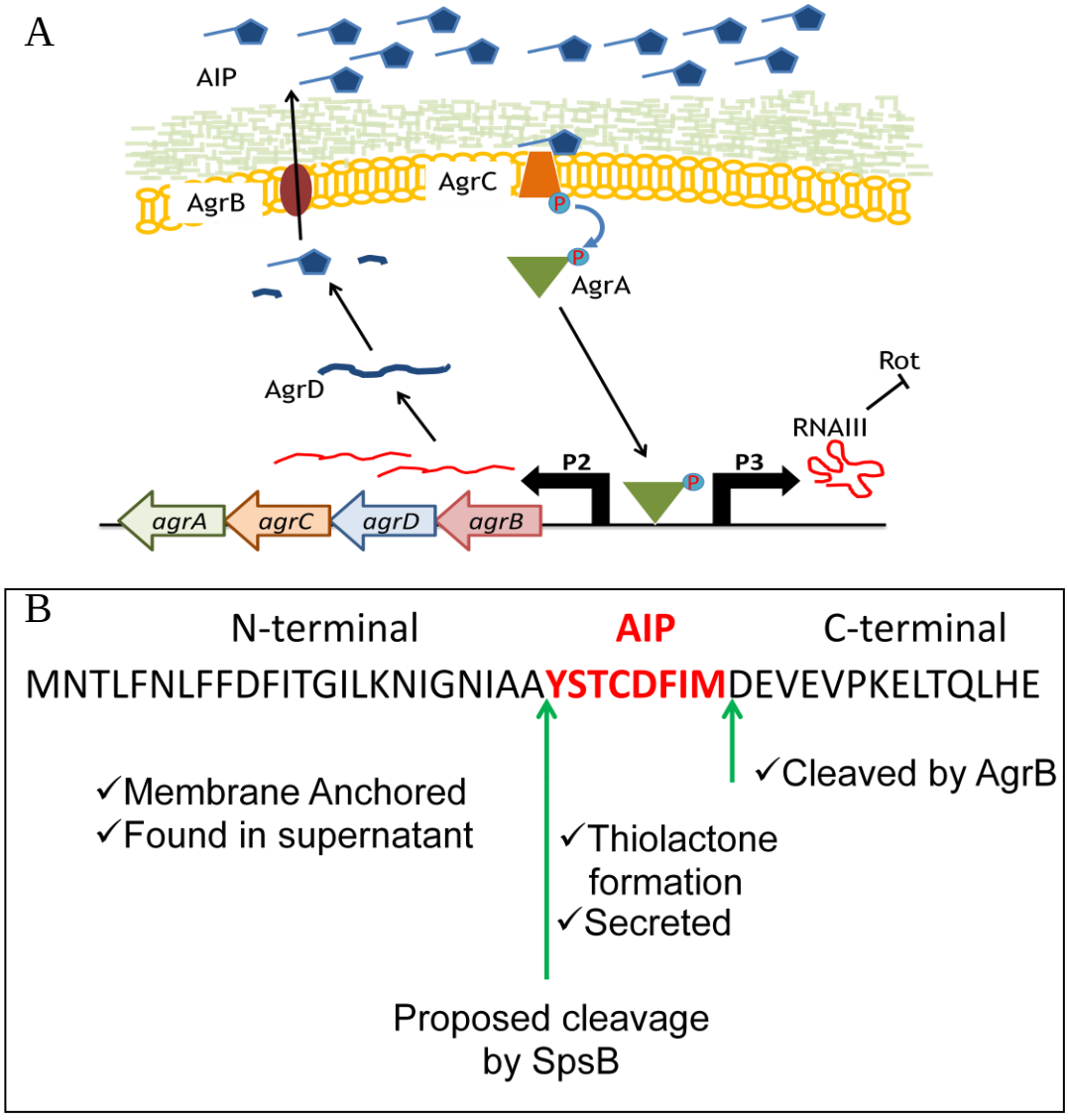

Figure 1. The accessory gene regulatory system in *S. aureus*. (A)The Agr quorum sensing system in *S. aureus* is comprised of: the autoinducing peptide precursor, AgrD; a protease involved in cleaving the C-terminal end of AgrD, AgrB; a histidine kinase, AgrC, and the transcription factor, AgrA. Modified from a figure made by Dr. Alonzo. (B) Depiction of posttranslational modifications of AgrD.

While much of the AIP biosynthesis pathway has been elucidated, the processing of the N-terminal end of AgrD remains unclear. A number of studies have concluded that AgrB does not perform N-terminal cleavage of AgrD (12, 18) and that peptide translocation occurs prior to the N-terminal cleavage event (21). Peptide translocation

prior to cleavage is supported by recent work that found the N-terminal end of AgrD is present in cell free supernatant and that these fragments have both cytotoxic and proinflammatory activities (22). In 2007, Kavanaugh et al (23) put forward the hypothesis that the Type I Signal Peptidase, SpsB, is the peptidase required for processing the N-terminus of AgrD. However, there are some caveats to their study that warrant further investigation of other possible peptidases as mediators of AgrD cleavage. First, the fixed concentration of AgrD peptide used to detect cleavage events was below the binding affinity for most peptidases. Second, the authors suggested SpsB is responsible for peptide cleavage based upon protease inhibitor studies that were not fully validated for blockade of protease activity. Due to these complications associated with specificity of protease inhibition, the authors were unable to eliminate the possibility that other peptidases might also be involved in cleaving AgrD; thus, they were unable to definitively ascribe a role for SpsB as the only peptidase involved in cleavage. Furthermore, when the authors generated a mutation in the AgrD peptide that would be predicted to inhibit SpsB activity, they were unable to prevent cleavage. In addition, a review by Wang et al (21) notes that currently only indirect evidence for a role of SpsB in peptide cleavage is indicated. Based on the methods used for this study and the evidence presented, we suggest that SpsB is not the only N-terminal modifier of AgrD. In this thesis, we hypothesize that another peptidase is responsible for processing the N-terminus of AgrD to generate AIP.

Once AgrD is processed and exported, the processed AIP accumulates in the extracellular space (Figure 1). As the concentration of AIP increases, the histidine kinase

AgrC recognizes the AIP, leading to AgrC activation. AgrC then phosphorylates and activates the response regulator, AgrA (14). AgrA is comprised of two domains, an N-terminal receiver domain that dimerizes and a C-terminal DNA binding domain with consensus DNA elements (24). Active AgrA then binds to the *P2* promoter to upregulate the remainder of the system. AgrA also binds to a promoter known as *P3,* which directly regulates virulence factor expression including genes encoding major toxins and hemolysins (9).

The Agr pathway affects expression of a wide range of virulence factors that facilitate pathogenesis. AgrA upregulates the transcription of a regulatory RNA known as RNAIII, which interacts with target mRNAs and either facilitates their degradation or increases their stability and translation efficiency (25, 26). One degradation target of RNAIII is the mRNA that encodes the transcription factor repressor of toxins, Rot (26). The down regulation of Rot translation by RNAIII leads to reduced production of surface proteins such as Protein A, the antibody binding protein used by *S. aureus* to resist phagocytosis as well as prevent B-cell receptor cross-linking (27). Protein A binds the Fcγ domain of IgG positioning the antibody in the incorrect orientation on the surface of *S. aureus* leading to decreased opsonization and phagocytosis efficiency (28, 29). Additionally, Protein A can bind to immunoglobulin on the surface of B cell receptors leading to clonal expansion resulting in apoptosis, thereby decreasing the amount of antibody produced (30). Furthermore, it has been shown that mice infected with a Protein A mutant have less kidney abscesses than mice infected with wild type *S. aureus* (28).

The down regulation of Rot by RNAIII also leads to increased expression of the toxins Rot normally represses which includes a diverse array of virulence factors. For example, the β-barrel pore–forming toxin, alpha toxin, is regulated by RNAIII and is used by *S. aureus* to lyse red blood cells and epithelial cells as well as modulate neutrophil functions (31). The alpha toxin binds to a host cell receptor, ADAM10, and forms a heptameric pore in host cell membranes leading to cell death (32). This toxin is crucial for the pathologic outcomes associated with skin and soft tissue infection and bacteremia, but is not required for early establishment of abscess lesions (31, 33, 34). Other examples of Agr regulated virulence factors are the leukotoxins AB and ED, which are involved in targeted destruction of leukocytes (35, 36), as well as the Phenol-soluble modulins (PSMs), a group of peptide toxins that are involved in red and white blood cell lysis (37), biofilm formation (38), and receptor-mediated inflammatory responses(39, 40). Recent research has shown that PSMs are vital for phagosomal escape, while LukAB is a major factor involved in inducing cell death and bacterial escape from macrophages, all functions that are required for bacterial survival and dissemination (41, 42).

The above examples only touch the surface of the considerable number and types of virulence factors, regulated by Agr, and contributing to *S. aureus* pathogenesis. Because of its broad capacity to alter the expression of such a wide range of virulence mediators, the Agr locus is one of the most extensively regulated loci in *S. aureus*. It receives additional regulatory inputs from many secondary regulators, including those with repressive functions to dampen imappropriate gene expression (7). These gene expression complexities are illustrated by the varied secondary inputs that alter RNAIII

expression in clinical isolates. For example, the primary infectious isolate in the United States, USA300, has higher levels of RNAIII compared to other lineages (7). It is suggested that the increased toxin production associated with increased steady-state RNAIII levels may provide an explanation for the enhanced virulence of this community-acquired MRSA strain (7). Thus, it is clear that the stringent regulation and interactions of protein products of the Agr system have the potential to dramatically influence clinical infection outcomes. Elucidating the precise mechanisms of Agr function is necessary for improving our understanding of *S. aureus* pathogenesis as well as allowing us to examine the Agr system as a possible drug target.

Abortive infectivity proteins and CAAX proteases in peptide processing.

Many bacterial species contain genes that encode a family of proteins known as abortive infectivity (Abi) proteins. Abi proteins are widely understood to facilitate self-immunity against phage infections through an array of mechanisms including delay of DNA replication or inhibition of phage protein synthesis (43). To prevent bacteriophage from spreading, some Abi proteins promote bacterial self-sacrifice to block propagation of an infection (43-45). Other Abi proteins contribute to surface protein display and cell division in *S. aureus* (45). In addition, some Abi proteins have been shown to function as metalloproteases involved in bacteriocin maturation, as is seen in *Lactobacillus plantarum* and *Streptococcus pneumonia* (46), while others function in toxin anti-toxin systems as well as bacteriocin self-immunity (46, 47). Clearly, there is a wide range of functions associated with Abi proteins despite their highly conserved motifs (48): two

glutamates, three additional residues, and an arginine (EEXXXR) as well as a second motif containing phenylalanine, three residues, and a histidine (FXXXH).

Abi protein domains are related to the CAAX protease family (48). The CAAX family is made up of metalloproteases that promote protein localization at the membrane by recognizing and prenylating a CAAX motif on the C-terminal end of their target protein (49). Prenylation is the process that covalently attaches lipid molecules to proteins to facilitate membrane localization. Similar to Abi proteins, other CAAX proteases have also been found to be involved in bacteriocin maturation and modification of small peptides (48). Because these proteins have such a wide range of functions, it is difficult to assign specific activities to an Abi or CAAX protein based on its conserved domains alone.

Preliminary studies conducted by Dr. Alonzo used a transposon mutant library to screen for secreted factors that elicited altered macrophage activation. One mutant that was identified had a diminished exoprotein profile compared to wild type *S. aureus* as well as elicited a heightened IL-1β response when supernatants from the mutant were applied to murine bone marrow derived macrophages. The *SAUSA300_1984* gene encodes a putative membrane spanning peptidase that is 247 amino acids in length and contains conserved Abi protein family motifs (Figure 2). Additionally, the protein encoded by the *1984* gene has ten predicted membrane-spanning domains with both its N-terminal end and its C-terminal end inside of the cell. When the function of 1984 was investigated alongside other proteins from *S. aureus* with conserved Abi domains, 1984 had no apparent role in surface protein display and cell division (45). However this study

only examined the surface display of Protein A in depth. 1984 also contains a predicted CAAX prenyl protease domain. It is currently unclear how these domains may play a role in the function of 1984. However, based on the homology to Abi proteins and CAAX proteases, I hypothesized 1984 may function as a peptidase and chose to investigate the role of 1984 in *S. aureus* peptide processing. Furthermore, based on the data provided from the transposon mutant library screen, 1984 might be involved in altering optimal macrophage responses and facilitating pathogenesis. The goal of the study described in this thesis was to define the role of 1984 in *S. aureus* quorum sensing and virulence during infection.

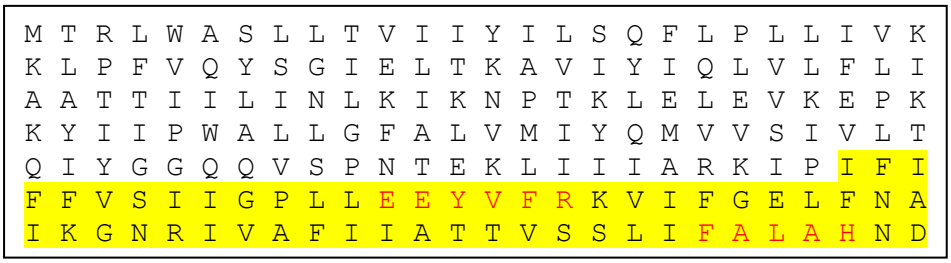

Figure 2. 1984 contains a conserved CAAX domain. The amino acid sequence of 1984 is shown. In red are conserved Abi motifs, while the CAAX domain hit is highlighted in yellow.

Conclusions.

S. aureus produces a wide range of virulence factors that promote evasion of immune surveillance mechanisms and promote survival during infection. The rise in *S. aureus* infection incidence is thought to be partially due to alterations in virulence factor gene expression allowing more efficient immune evasion. Furthermore, *S. aureus* uses complex regulatory systems, including the Agr quorum sensing system, during the course of infection to promote survival. Given my identification of 1984, a novel Abi-like

protein that modulates macrophage activation and has defects in protein secretion, I sought to define its role in facilitating pathogenesis in *S. aureus*.

CHAPTER TWO

MATERIALS AND METHODS

Bacterial strains and culture conditions.

For the purposes of this study, all recombinant plasmids were passaged through *E. coli* before propagation in *S. aureus. E. coli* DH5α was used for most plasmid propagation. When constructing a *1984* complementation vector, I found that *1984* was toxic in *E. coli*, therefore *E. coli* BH10C was used as a host strain; BH10C reduces copy number of plasmids to near single-copy levels to limit expression of the toxic gene in *E. coli* (50). Once passaged through *E. coli, S. aureus* RN4220 or RN9011 (RN4220+pRN7023) were used as intermediate strains that are amenable to DNA uptake. Following propagation in one of these strains plasmids could then be introduced into clinical isolates. *S. aureus* LAC (AH-1263) was used as the wild type strain for this study. LAC (AH-1263) is a *S. aureus* USA300 isolate cured of its plasmids (51). All strains used and constructed in this work are described in Table 1. All *E. coli* strains were grown in Lysogeny Broth (LB) (Amresco), while *S. aureus* strains were grown in either a rich medium, Tryptic Soy Broth (TSB) (Criterion), or defined medium, Roswell Park Memorial Institute medium (RPMI) (corning) supplemented with 1% casamino acids (Amresco) and 2.4 mM Sodium bicarbonate (Amresco). These two different media were used because *S. aureus* can differentially regulate gene expression upon culture in either medium. Additionally, antibiotics were used when necessary for

plasmid selection as well as mutagenesis protocols. Media were supplemented with antibiotics at the following concentrations: ampicillin (Amp) at 100μg/mL, erythromycin (Erm) at 10 μg/mL, chloramphenicol (Cm) at 10 μg/mL, anhydrous tetracycline (AnTet) (Acròs Organics) at 1 μg/mL, and tetracycline (Tet) at 10 μg/mL (Amresco and Acròs Organics). In order to monitor bacterial growth, optical density at 600 nm (OD600) was measured using a Genesys 10S UV-Vis spectrophotometer (Thermo).

Strain	**Description**	**Designation**	**Source/ Reference**
AH-1263	*S. aureus* USA300 Strain LAC. Plasmid cured.	LAC (WT)	(51)
DH5α	*E. coli* strain for recombinant plasmids	DH5α	
BH10C	*E. coli* strain that restricts plasmid copy number for complementation of *1984*	BH10C	(50)
RN4220	Restriction deficient *S. aureus*	RN4220	(52)
RN9011	RN4220+ pRN7023 exressing SaPI1 Integrase	RN9011	(53)
FA-S922	LAC (AH-1263 – plasmid cured) with an in-frame deletion of *1984*	Δ*1984*	This work
FA-S982	FA-S922 complemented with pJC1112-*1984*	Δ*1984+1984*	This work
	LAC gene replacement mutant of *agrBDCA* with tetracylcine resistance cassette	Δ*agr::tet*	
FA-S1008	LAC (AH-1263) gene replacement mutant of *agrBDCA* with tetracylcine resistance cassette	Δ*agr::tet*	This work
FA-S995	FA-S922 transduced with Δ*agr::tet* mutation	Δ*1984* Δ*agr::tet*	This work
AH-E462	*E. coli* containing reporter plasmid pDB59 with *gfp* expression driven by the *P3* promoter		(54)
FA-S945	FA-S922 with GFP reporter plasmid pDB59	Δ*1984*+pDB59	This work
FA-S949	LAC (AH-1263) with GFP reporter plasmid pDB59	WT+pDB59	This work
FA-S984	LAC Δ*agr* with GFP reporter plasmid pDB59	Δ*agr*+pDB59	This work
FA-S1009	LAC (AH-1263) with pJC1112-*agrBD* w/ N terminal *6x-His*	WT+*6xHis-agrBD*	This work
FA-S1011	FA-S995 with pJC1112-*agrBD* w/ N terminal *6x-His*	Δ*1984* Δ*agr+6xHis-agrBD*	This work
FA-S1013	FA-S1008 with pJC1112-*agrBD* w/ N terminal *6x-His*	Δ*agr+6xHis-agrBD*	This work
FA-S1014	FA-S922 with pJC1112-*agrBD* w/ N terminal *6x-His*	Δ*1984+6xHis-agrBD*	This work
FA-S1027	LAC (AH-1263) with pJC1112-*agrBD* w/ C terminal *6x-His*	WT+*agrBD-6xHis*	This work

FA-S1029	FA-S922 with pJC1112-*agrBD* w/ C terminal *6x-His*	Δ*1984*+ *agrBD-6xHis*	This work
FA-S1082	FA-S995 containing pOS1-P_{hrt}-*agrD* with a *6x-His*-tag on the C-terminal end. This is a hemin inducible promoter.	Δ*1984* Δ*agr*+ pOS1-P_{hrt}-*agrD+6xHis*	This work
FA-S1083	FA-S1008 containing pOS1-P_{hrt}-*agrD* with a *6x-His*-tag on the C-terminal end	Δ*agr* +pOS1-P_{hrt}-*agrD-6xHis*	This work
FA-S1084	FA-S995 containing pOS1-P_{hrt}-*agrD* with a *6x-His*-tag on the N-terminal end.	Δ*1984* Δ*agr* +pOS1-P_{hrt}-*6xHis-agrD*	This work
FA-S1085	FA-S1008 containing pOS1-P_{hrt}-*agrD* with a *6x-His*-tag on the N-terminal end	Δ*agr*+pOS1-P_{hrt}-*6xHis-agrD*	This work
FA-S1086	LAC (AH-1263) containing pOS1-P_{hrt}-*agrD* with a *6x-His*-tag on the C-terminal end	WT+pOS1-P_{hrt}-*agrD-6xHis*	This work
FA-S1087	FA-S922 containing pOS1-P_{hrt}-*agrD* with a *6x-His*-tag on the C-terminal end	Δ*1984*+pOS1-P_{hrt}-*agrD-6xHis*	This work
FA-S1088	LAC (AH-1263) containing pOS1-P_{hrt}-*agrD* with a *6x-His*-tag on the N-terminal end	WT+pOS1-P_{hrt}-*6xHis-agrD*	This work
FA-S1089	FA-S922 containing pOS1-P_{hrt}-*agrD* with a *6x-His*-tag on the N-terminal end	Δ*1984*+pOS1-P_{hrt}-*6xHis-agrD*	This work
FA-S1092	LAC (AH-1263) containing pOS1-P_{lgt}-*agrD* with *6x-His*-tag on the N-terminal end	WT+pOS1-P_{lgt}-*6xHis-agrD*	This work
FA-S1093	FA-S922 containing pOS1-P_{lgt}-*agrD* with *6x-His*-tag on the N-terminal end	Δ*1984*+pOS1-P_{lgt}-*6xHis-agrD*	This work
FA-S1094	FA-S1008 containing pOS1-P_{lgt}-*agrD* with *6x-His*-tag on the N-terminal end	Δ*agr*+pOS1-P_{lgt}-*6xHis-agrD*	This work
FA-S1095	FA-S995 containing pOS1-P_{lgt}-*agrD* with *6x-His*-tag on the N-terminal end	Δ*1984* Δ*agr*+pOS1-P_{lgt}-*6xHis-agrD*	This work
FA-S1096	LAC (AH-1263) containing pOS1-P_{lgt}-*agrD* with *6x-His*-tag on the C-terminal end	WT+pOS1-P_{lgt}-*agrD-6xHis*	This work
FA-S1097	FA-S922 containing pOS1-P_{lgt}-*agrD* with *6x-His*-tag on the C-terminal end	Δ*1984*+pOS1-P_{lgt}-*agrD-6xHis*	This work
FA-S1098	FA-S1008 containing pOS1-P_{lgt}-*agrD* with *6x-His*-tag on the C-terminal end	Δ*agr*+pOS1-P_{lgt}-*agrD-6xHis*	This work
FA-S1099	FA-S995 containing pOS1-P_{lgt}-*agrD* with *6x-His*-tag on the C-terminal end	Δ*1984* Δ*agr*+pOS1-P_{lgt}-*agrD-6xHis*	This work
FA-S1133	LAC (Ah-1263) containing pOS1-P_{HELP}-agrD with *6x-His*-tag on the N-terminal end	WT+pOS1-P_{HELP}-*6xHis-agrD*	This work
FA-S1134	FA-S922 containing pOS1-P_{HELP} -*agrD* with *6x-His*-tag on the N-terminal end	Δ*1984*+pOS1-P_{HELP}-*6xHis-agrD*	This work
FA-S1135	FA-S1008 containing pOS1- P_{HELP} -*agrD* with *6x-His*-tag on the N-terminal end	Δ*agr*+pOS1-P_{HELP}-*6xHis-agrD*	This work
FA-S1136	FA-S995 containing pOS1- P_{HELP} -*agrD* with *6x-His*-tag on the N-terminal end	Δ*1984* Δ*agr*+pOS1-P_{HELP}-*6xHis-agrD*	This work
FA-S1137	LAC (Ah-1263) containing pOS1-P_{HELP} -*agrD* with *6x-His*-tag on the C-terminal end	WT+pOS1-P_{HELP}-*agrD-6xHis*	This work
FA-S1138	FA-S922 containing pOS1-P_{HELP} -*agrD* with *6x-His*-tag on the C-terminal end	Δ*1984*+pOS1-P_{HELP}-*agrD-6xHis*	This work
FA-S1139	FA-S1008 containing pOS1-P_{HELP} -*agrD* with *6x-His*-tag on the C-terminal end	Δ*agr*+pOS1-P_{HELP}-*agrD-6xHis*	This work
FA-S1140	FA-S995 containing pOS1-P_{HELP} -*agrD* with *6x-His*-tag on the C-terminal end	Δ*1984* Δ*agr*+pOS1-P_{HELP}-*agrD-6xHis*	This work

FA-S1141	LAC (AH-1263) containing pOS1-P_{sarA}- sod_{RBS} -*agrD* with *6x-His*-tag on the N-terminal end	WT+ pOS1-P_{sarA}- sod_{RBS} *-6xHis-agrD*	This work
FA-S1142	FA-S922 containing pOS1-P_{sarA}- sod_{RBS} *-agrD* with *6x-His*-tag on the N-terminal end	Δ*1984*+ pOS1-P_{sarA}- sod_{RBS} *-6xHis-agrD*	This work
FA-S1143	FA-S1008 containing pOS1-P_{sarA}- sod_{RBS} *-agrD* with *6x-His*-tag on the N-terminal end	Δ*agr*+ pOS1-P_{sarA}- sod_{RBS} *-6xHis-agrD*	This work
FA-S1144	FA-S995 containing pOS1-P_{sarA}- sod_{RBS} *-agrD* with *6x-His*-tag on the N-terminal end	Δ*1984* Δ*agr*+ pOS1-P_{sarA}- sod_{RBS} *-6xHis-agrD*	This work
FA-S1145	LAC (AH-1263) containing pOS1-P_{sarA}- sod_{RBS} -*agrD* with *6x-His*-tag on the C-terminal end	WT+ pOS1-P_{sarA}- sod_{RBS} *-agrD-6xHis*	This work
FA-S1146	FA-S922 containing pOS1-P_{sarA}- sod_{RBS} *-agrD* with *6x-His*-tag on the C-terminal end	Δ*1984*+ pOS1-P_{sarA}- sod_{RBS} *-agrD-6xHis*	This work
FA-S1147	FA-S1008 containing pOS1-P_{sarA}- sod_{RBS} *-agrD* with *6x-His*-tag on the C-terminal end	Δ*agr*+ pOS1-P_{sarA}- sod_{RBS} *-agrD-6xHis*	This work
FA-S1221	FA-S995 containing pOS1-P_{sarA}- sod_{RBS} *-agrD* with *6x-His*-tag on the C-terminal end	Δ*1984* Δ*agr*+ pOS1-P_{sarA}- sod_{RBS} *-agrD-6xHis*	This work
FA-S1265	FA-S982 containing pOS1-P_{sarA}- sod_{RBS} *-agrD* with *6x-His*-tag on the C-terminal end	Δ*1984+1984*+ pOS1-P_{sarA}- sod_{RBS} *-agrD-6xHis*	This work
FA-E1165	E. coli (LysY/Iq) containing *pET-41b-AgrD*		This work
FA-S1297	LAC (AH-1263) containing pOS1-P_{sarA}- sod_{RBS} -*6xHis* with a 45 amino acid linker before *agrD-cmyc*	WT+ pOS1-P_{sarA}- sod_{RBS} *-6xHis-link-agrD*	This work
FA-S1298	FA-S922 containing pOS1-P_{sarA}- sod_{RBS} *-6xHis* with a linker before *agrD-cmyc*	Δ*1984*+ pOS1-P_{sarA}- sod_{RBS} *-6xHis-link-agrD*	This work
FA-S1299	FA-S982 containing pOS1-P_{sarA}- sod_{RBS} *-6xHis* with a linker before agrD-cmyc	Δ*1984+1984*+ pOS1-P_{sarA}- sod_{RBS} -6xHis-link-*agrD*	This work
FA-S1300	FA-S1008 containing pOS1-P_{sarA}- sod_{RBS} *-6xHis* with a linker before *agrD-cmyc*	Δ*agr*+ pOS1-P_{sarA}- sod_{RBS} *-6x-His-link-agrD*	This work
FA-S1301	FA-S995 containing pOS1-P_{sarA}- sod_{RBS} *-6xHis* with a linker before *agrD-cmyc*	Δ*1984* Δ*agr*+ pOS1-P_{sarA}- sod_{RBS} *-6xHis-link-agrD*	This work

Table 1. List of strains used in this study.

Molecular genetics techniques.

To isolate genomic DNA from *S. aureus*, cultures were grown overnight in 5 mL TSB at 37°C with shaking at 200 rpm. 1.5 mL of bacteria were then pelleted by centrifugation and resuspended in 200 µL of TSM buffer (50 mM Tris, 0.5 M Sucrose, 10 mM MgCl2 (pH 7.5)) and 2.5 µL of a lysostaphin (Ambi Products) stock for a final concentration of 25 µg/mL. Samples were mixed and incubated at 37°C for 15 minutes to digest the cell wall of *S. aureus*. After this treatment the bacteria were pelleted by

centrifugation at 14000 rpm for 5 minutes, supernatants were discarded, and the genomic DNA was isolated using a Wizard Genomic DNA purification kit (Promega). Polymerase chain reaction (PCR) was performed in a Flexid Mastercycler (eppendorf) using Phusion High-Fidelity DNA Polymerase (New England Biolabs) or GoTaq DNA Polymerase (Promega) and dNTPs (Quanta Biosciences). For all PCR reactions oligonucleotides were ordered from Eurofins (see Table 2). Electrophoresis of DNA samples was performed in 0.8% agarose (Amresco) gels. Digestions were performed using restriction endonucleases: XhoI, BamHI, EcoRI, KpnI, SacI and PstI (New England Biolabs) following the manufacturer's suggested protocols and digested plasmids were treated with Shrimp Alkaline Phosphatase (Amresco). Following digestion, ligations were set up using T4 DNA Ligase (New England Biolabs) and were incubated in an eppendorf ThermoMixer at 16°C overnight. When necessary, PCR purifications and DNA gel extractions were carried out using QIAGEN QIAquick kits.

Name	**Sequence**
1984-1 KpnI	CCC-**GGTACC (KpnI)**-CCATAAATGATAAACCTCCAT
1984-2	GTGTGATTCGTTTTTTTTATTA-**GGCGCC**-CATAATTTTCCTCCAAATATT
1984-3	AATATTTGGAGGAAAATTATG-**GGCGCC**-TAATAAAAAAAACGAATCACAC
1984-4 SacI	CCC-**GAGCTC (SacI)**-ATTTTTAGCCTTGGCAAATG
37F	GGCGGATCCAGCACTATCAGTTAAAACAAT
37R	GGCGAATTCACAAGAAGATAATAAGAAAAG
agrB-F	ATAT-**GGATCC(BamHI)**-ATGTTAAAATATTAAATACAAATT
agrB-R	AAATAAGTTAAATAATGTATT-GTGATGGTGATGGTGATG-CATTTTAAGTCCTCCTTAATA
agrD-F	TATTAAGGAGGACTTAAAATG-CATCACCATCACCATCAC-AATACATTATTTAAACTTATTT
agrD-R	ATAT-**GAATTC(EcoRI)**-TTATTCGTGTAATTGTGTTAA
agrD-6xHis-R	ATAT-**GAATTC(EcoRI)** TTAGTGATGGTGATGGTGATGTTCGTGTAATTGTGTTAATTC
6xHis-agrD-F XHOI	ATAT- **CTCGAG (XHOI)**-ATGCATCACCATCACCATC
6xHis-agrD-R EcoRI	ATAT-**GAATTC (EcoRI)**-TTATTCGTGTAATTGTGTTAAT
agrD-6xHis-F-XhoI	ATAT-**CTCGAG (XHOI)**-ATGAATACATTATTTAACTTATTT

agrD-6xHis-R-EcoRI	ATAT-**GAATTC(ecorI)**-TTAGTGATGGTGATGGTGA
6xHis-agrD-R-BamHI	ATAT-**GGATCC(BamHI)**- TTATTCGTGTAATTGTGTTAAT
agrD-6xHis-R-BamHI	ATAT-**GGATCC(BamHI)**- TTAGTGATGGTGATGGTGA
P_{HELP}-*agrD*-SOE1-PstI	ATAT-**CTGCAG(PSTI)**-ATCCCATTATGCTTTGGCA
P_{HELP}-*6xHis-agrD*-SOE2	GATGGTGATGGTGATGCAT-GGGTTTCACTCTCCTTCTA
P_{HELP}-*6xHis-agrD*-SOE3	TAGAAGGAGAGTGAAACCC-ATGCATCACCATCACCATC
P_{HELP}-*6xHis-agrD*-SOE4-BamHI	ATAT-**GGATCC(BamHI)**-TTATTCGTGTAATTGTGTTAAT
P_{HELP}-*agrD-6xHis*-SOE2	AAATAAGTTAAATAATGTATTCAT-GGGTTTCACTCTCCTTCTA
P_{HELP}-*agrD-6xHis*-SOE3	TAGAAGGAGAGTGAAACCC-ATGAATACATTATTTAACTTATTT
P_{HELP}-*agrD-6xHis*-SOE4-BamHI	ATAT-**GGATCC(BamHI)**-TTAGTGATGGTGATGGTGA
P_{sara}- sod_{RBS} -SOE1-PstI	ATAT-**CTGCAG(pstI)**-CTGATATTTTTGACTAAACCA
P_{sara}- sod_{RBS} -*6xHis-agrD*-SOE2	GATGGTGATGGTGATGCAT-AAATAATCATCCTCCTAAGG
P_{sara}- sod_{RBS} -*6xHis-agrD*-SOE3	CCTTAGGAGGATGATTATTT-ATGCATCACCATCACCATC
P_{sara}- sod_{RBS} -*6xHis-agrD*-SOE4-EcoRI	ATAT-**GAATTC(ecorI)**-TTATTCGTGTAATTGTGTTAAT
P_{sara}- sod_{RBS} -*agrD-6xHis*-SOE2	AAATAAGTTAAATAATGTATTCAT-AAATAATCATCCTCCTAAGG
P_{sara}- sod_{RBS} -*agrD-6xHis*-SOE3	CCTTAGGAGGATGATTATTT-ATGAATACATTATTTAACTTATTT
P_{sara}- sod_{RBS} -*agrD-6xHis*-SOE4-EcorI	ATAT-**GAATTC(ecorI)**-TTAGTGATGGTGAATGGTGA
UNI- P_{sara}- sod_{RBS} -SOE1-PstI	ATAT-**CTGCAG(Pst1)**-CTGATATTTTTGAC
P_{sara}- sod_{RBS} -*6xHis-Linker-agrD*-SOE2	GATGACCAGAACCACTAGT-CATAAATAATCATCCTCCTAAGGT
P_{sara}- sod_{RBS} -*6xHis-Linker-agrD*-SOE3	ACCTTAGGAGGATGATTATTT-ATGACTAGTGGTTCTGGTCATC
P_{sara}- sod_{RBS} -*6xHis-Linker-agrD*-SOE4-EcorI	ATAT-**GAATTC** (ecorI)-CTCGAG(XhoI)-CAGATCTTCTTCA

Table 2. List of Oligonucleotides

To isolate plasmids from *S. aureus*, 5 mL overnight cultures of bacteria were grown in TSB at 37°C with shaking at 200 rpm. The next day, bacteria were pelleted by centrifugation at 4200 rpm for 15 minutes and then resuspended in 400µl of TSM buffer and 20 µl of lysostaphin stock solution for a final concentration of 0.1 mg/mL of

lysostaphin. Samples were incubated for 10 minutes at 37°C. After digesting the cell wall with lysostaphin, the bacteria were centrifuged at 13000 rpm for 2 minutes and supernatants were discarded. A Qiagen miniprep kit was used to isolate plasmid DNA. DNA was eluted with sterile water in all cases. DNA sequencing was performed by Genscript.

***E. coli* competent cell preparation.**

To prepare chemically competent *E. coli*, 3 mL overnight cultures were grown in LB at 37°C with shaking at 200 rpm. The next day, sub-cultures were inoculated at a 1:55 dilution in 110 mL fresh LB. Bacteria were incubated at 37°C with shaking at 200 rpm until the cultures reached mid-logarithmic phase, OD600 nm 0.3 -0.4 (about 2.5 hours). Upon reaching logarithmic growth phase, the culture was distributed into four 50 mL conical tubes and chilled on ice for 10 minutes. Samples were then centrifuged at 4000 rpm for 5 minutes at 4°C, supernatants were discarded, and pellets were resuspended in 10 mL of Transfomation Buffer 1 (30 mM KOAc, 100 mM $RbCl_2$, 10 mM $CaCl_2$, 50 mM $MnCl_2$, 15% Glycerol (pH 5.8)(Amresco)). Cells were incubated on ice for 10 minutes and then centrifuged at 4000 rpm for 5 minutes at 4°C, supernatants were discarded, and pellets were resuspended in 1 mL of filter-sterilized Transformation Buffer 2 (10 mM MOPS, 10 mM $RbCl_2$, 75 mM $CaCl_2$, 15% Glycerol (pH 6.5)(Amresco)). Once resuspended, cells were aliquoted into 1.5 mL microcentrifuge tubes and stored at -80°C.

***E. coli* heat transformation.**

Chemically competent cells were thawed on ice before being mixed with 5 μL of a ligation mixture and incubated on ice for 30 minutes. After 30 minutes, cells were heat

shocked for 45 seconds at 42°C and immediately put back on ice for an additional 2 minutes. 250 μL of sterile SOC medium [2% tryptone (Amresco), 0.5 % yeast extract (Amresco), 0.05 % NaCl (Amresco), 10% 250 mM KCl (Amresco), and 20% filter-sterilized 1 M glucose solution (pH 7.0)] was added to the transformation mixture and incubated at 37°C, with shaking at 200 rpm, for 2 hours. Following this incubation, 50 μL of competent cells were spread onto LB plates containing any required antibiotics for selection and placed at 37°C overnight. Colonies were then screened for antibiotic resistance and the presence of the transformed plasmid.

Preparation of *S. aureus* electrocompetent cells.

S. aureus cultures were grown overnight in 5 mL of TSB with any required antibiotics at 37°C with shaking at 200 rpm. The next day, the cultures were diluted 1:100 in 30 mL of fresh TSB and incubated for 3 hours until reaching mid-logarithmic phase. After 3 hours the bacteria were pelleted by centrifugation at 8000 rpm for 10 minutes at 4°C and the supernatants were discarded. The pellet was resuspended in 30 mL of ice-cold 10% glycerol (Amresco) and then centrifuged and washed two additional times, first in 30 mL of 10% glycerol and then 15 mL of 10% glycerol. After a final spin, cells were resuspended in 3 mL 10% glycerol and aliquots were stored in 1.5 mL microcentrifuge tubes at -80°C until needed.

***S. aureus* transformation.**

To transform plasmids into *S. aureus* strains via electroporation, 3 μL to 10 μL of purified plasmid was incubated with 50 μL of competent *S. aureus* cells that were thawed at room temperature for 5 minutes. The mixture was incubated at room temperature for 30 minutes before being transferred to a sterile 2 mm electropoation cuvette (VWR).

Samples were electroporated (pulsed at 1800 V, 10 μF, and 600 Ω) in a GenePulser Xcell BIORAD Electroporator. Immediately following electroporation, 750 μL of fresh TSB was added to the samples and cells were then transferred to microcentrifuge tubes and incubated at 30°C. Following recovery, either 100 μL of cells were spread on TSA plates or samples were centrifuged at 10000 rpm for 2 minutes and all but 100 μL were removed from the supernatant and the cells were resuspended in 100 μL followed by spreading on TSA plates. Plates were supplemented with antibiotics as needed for selection and subsequently incubated at 30°C or 37°C overnight. Occasionally, samples required 24-48 hours for bacterial growth to be observed. Colonies were then screened for antibiotic resistance and plasmid presence.

Bacteriophage-mediated generalized transduction.

Transduction was used to stably integrate plasmids, as well as generate marked mutations within the *S. aureus* chromosome. *S. aureus* specific bacteriophages ϕ11 or 80α were used in this study. Donor strains were grown overnight in 3 mL of TSB/LB (1:1) supplemented with 5 mM calcium chloride ($CaCl_2$)(Amresco) and 5 mM magnesium sulfate ($MgSO_4$)(Amresco) at 37°C with shaking at 200 rpm. The next day, overnight cultures were diluted 1:100 in 10 mL of fresh TSB/LB (1:1), again supplemented with 5 mM $CaCl_2$ and 5 mM $MgSO_4$. Samples were grown for about 3 hours at 37°C with shaking at 200 rpm until the cultures reached an optical density (OD 600 nm) between 0.3 and 0.9. To package the donor DNA into the phage, 100 μL of 10-fold serial dilutions (10^{-1} to 10^{-10}) of bacteriophage stock in TMG (10 mM Tris pH 7.5, 5 mM $MgCl_2$, 0.01% gelatin (v/v)) were added to 15 mL conical tubes and incubated with 500 μL of the donor *S. aureus* culture. The phage-bacteria mixture was gently vortexed

and incubated at room temperature for 30 minutes. 2.5 mL of melted and cooled CY Top agar (Casamino acids 5 g/L, Yeast Extract 5 g/L, glucose 5 g/L, NaCl 6 g/L, 7.5 g/L agar) supplemented with 5 mM $CaCl_2$ and 5 mM $MgSO_4$ was quickly added to each tube. The mixture of CY top agar, bacterial suspension, and the phage dilutions were immediately poured onto TSA plates. Plates were incubated overnight at 30°C. The following day, phage were harvested from two to three plates with confluent plaques. The top agar was scraped from each of these plates using a sterile scoopula and combined into one 50 mL conical tube. 2 mL of TMG buffer per plate was added to the tube and vortexed extensively. To separate the agar from the bacteriophage, the tube was centrifuged for 15 minutes at maximum speed. The supernatant was collected and filter sterilized once through a 0.45 μm syringe filter and twice through a 0.22 μm syringe filter. Bacteriophage stocks were stored at 4°C.

To transduce plasmids and marked mutations, recipient strains were first grown overnight in 20 mL of TSB/LB (1:1) supplemented with 5 mM $CaCl_2$ at 37°C. Samples were then centrifuged for 15 minutes at max speed, supernatants were discarded, and the pellets were resuspended in 3 mL of CY medium (casamino acids 5 g/L, yeast extract 5 g/L glucose 5 g/L NaCl 6 g/L) supplemented with 5 mM $CaCl_2$. Next, 4 conditions were set up with bacteria alone or 10-fold serial dilutions of bacteria infected with 100 μL of bacteriophage stock packaged with donor DNA. Tubes were mixed by inverting every ten minutes for 30 minutes at room temperature. Next, 40 mM sodium citrate was added to each tube and incubated at room temperature for 30 minutes, again mixing every 10 minutes. Tubes were centrifuged at maximum speed for 5 minutes and washed twice in 500 μL of CY medium supplemented with 40 mM sodium citrate. After one final

centrifugation, samples were resuspended in 200 μL of CY medium supplemented with 40 mM sodium citrate and spread on CY agar or TSA plates containing 10 mM sodium citrate and any antibiotics necessary for selection. Plates were placed at 37°C overnight and potential transductants were screened for antibiotic resistance and acquisition of desired mutations.

Generation of a *SAUSA300_1984* in-frame deletion mutant.

A *SAUSA300_1984* in-frame deletion mutant was generated using a temperature-sensitive mutagenesis vector known as pIMAY (55). Two fragments that correspond to ~500 base pair regions of sequence homology immediately upstream and downstream of *1984* were amplified. Oligonucleotides 1984-1 and 1984-2 were used to amplify the region upstream of *1984*, while oligonucleotides 1984-3 and 1984-4 were used to amplify the region downstream of *1984* (Table 2). These fragments were joined by splicing by overlap extension (SOEing) PCR using oligonucleotides 1984-1 and 1984-4 and subcloned into the multi-cloning site of pIMAY using restriction endonucleases KpnI and SacI followed by ligation. pIMAY is a temperature sensitive plasmid that replicates at 28°C, but cannot replicate at 37°C and integrates into the *S. aureus* genome based upon recognition of overlap with the cloned regions of homology described above. Integration of pIMAY is selected on chloramphenicol plates as pIMAY contains a highly expressed chloramphenicol resistance gene. Once pIMAY-*1984* was transformed into LAC (AH-1263) by electroporation cultures were grown at 37°C in the presence of chloramphenicol, causing the plasmid to insert into the chromosome by recombination either upstream or downstream of *1984*. To facilitate a second recombination event that would promote plasmid excision and gene deletion, cultures were shifted to 28°C in the

absence of antibiotic selection. Following plasmid excision, inducible counter-selection with anhydrous tetracycline (AnTet) was used to eliminate *S. aureus* still harboring pIMAY by plating on medium containing AnTet. AnTet induces the expression of a *secY* antisense RNA transcript under control of the $P_{xyl/tetO}$ promoter. After curing the plasmid, potential mutants were screened by PCR using oligonucleotides 1984-1 and 1984-4 which flank the deleted region. The PCR products were run on an agarose gel and evaluated for a reduction in product length corresponding to deletion of the *1984* gene.

Generation of *1984* complementation strain.

A single copy chromosomal complementation strain was constructed using the pJC1112 vector, which stably integrates into a neutral site of the chromosome, driving *1984* expression under its native promoter (53). This construct was generated by PCR using oligonucleotides 37F and 37R (Table 2). The resulting amplicon was then subcloned into the pJC1112 vector using the EcoRI and BamHI restriction sites. This construct was then transformed into the DH5α *E. coli* followed by electroporation into the RN9011 where the plasmid integrates at the SapI1 site. The integrated complementation vector was then transduced into Δ*1984*. Complementation was confirmed by PCR and sequencing.

Construction of Δ*agr*::*tet* mutants.

A marked deletion mutation of *agrBDCA* was moved from a LAC background into plasmid cured LAC (AH-1263) as well as Δ*1984* by bacteriophage-mediated transduction, using phage 80α, as described above.

Construction of *P3* reporter strains.

The pDB59 plasmid described in Table 1 contains the *P3* promoter of the Agr system driving the expression of GFP. The *P3* promoter is induced when AgrA is activated by AIP-bound AgrC. Therefore, the plasmid monitors induction of the Agr system by AIP (54). The pDB59 plasmid was isolated from *E. coli* and passaged through RN4220. The plasmid was then electroporated into WT, Δ*1984,* and Δ*agr::tet.*

Construction of 6x-histidine-tagged AgrD expression vectors.

Construction of 6x-histidine-tagged AgrD with expression under its native promoter. We first constructed a series of 6x-histidine-tagged expression vectors using pJC1112 (used for complementing *1984*). These constructs drive *agrD* expression under its native promoter and therefore included the *agrB* gene. Constructs with a N-terminal 6x-histidine-tagged AgrD as well as a construct with a C-terminal 6x-histidine-tagged AgrD were created. For the N-terminal 6x-histidine-tagged construct (pJC1112-*agrB-6xHis-agrD*), two fragments corresponding to *agrB* and *agrD* were amplified. Oligonucleotides *agrB*-F and *agrB*-R were used to amplify *agrB,* while oligonucleotides *agrD*-F, which includes a 6x-histidine-tag coding sequence, and *agrD*-R were used to amplify the N-terminal 6x-histidine-tagged *agrD.* These fragments were joined by splicing by overlap extension (SOEing) PCR using oligonucleotides *agrB*-F and *agrD-R*. For the C-terminal tagged (pJC1112-*agrBD-6xHis*) construct, oligonucleotides *agrB*-F and *agrD-6xHis*-R, which includes a 6x-histidine-tag coding sequence were used. Once 6x-histidine-tagged *agrBD* amplicons were generated they were cloned into pJC1112 using EcoRI and BamHI restriction sites. Constructs were transformed into DH5α,

electroporated into RN9011, and transduced into wild type, Δ*1984,* Δ*1984+1984*, and Δ*agr* as described above.

Construction of inducible expression vector of 6x-histidine-tagged AgrD. All further 6x-His-tagged AgrD expression vectors used a pOS1 vector (56), which is a multicopy plasmid used to overcome issues of limited detection due to low protein abundance. Two constructs were created using a hemin inducible promoter, P_{hrt}, to drive expression of the N- or C- terminal 6x-histidine-tagged AgrD. The N-terminal tagged AgrD construct was PCR amplified from the pJC1112-*agrB-6xHis-agrD* construct as a template using oligonucleotides XhoI-*6xHis-AgrD* and *6xHis-AgrD*-EcoRI. The C-terminal tagged AgrD construct was amplified using pJC1112-*agrBD-6xHis* as a template and oligonucleotides XhoI-*AgrD-6xHis* and *AgrD-6xHis*-EcorI. Once cloned into the pOS1-P_{hrt} vector using the XhoI and EcoRI restriction sites, the constructs were transformed into DH5α, electroporated into RN4220, and then electroporated into wild type, Δ*1984,* Δ*1984+1984*, and Δ*agr* as described above.

Construction of constitutively expressed 6x-histidine-tagged AgrD driven by P_{lgt}. Similarly, both N and C-terminal 6x-histidine-tagged constructs were cloned into pOS1 under control of the P_{lgt} promoter, which is constitutive. For the N-terminal 6x-histidine-tagged construct the pJC1112-*agrB-6xHis-agrD* was used as the template in a PCR with oligonucleotides *6xHis-agrD*-F-XHOI and *6xHis-agrD*-R-BamHI. The C-terminal 6x-histidine-tagged construct used the pJC1112-*agrBD-6xHis* as the template for a PCR reaction using oligonucleotides *agrD-6xHis*-F-XhoI and *agrD-6xHis*-R-BamHI. These amplicons were then cloned into the XhoI and BamHI restriction sites of

the pOS1-P_{lgt} vectors and transformed into DH5α, electroporated into RN4220, and then electroporated into wild type, Δ*1984,* Δ*1984+1984,* and Δ*agr* as described above.

Construction of constitutively expressed 6x-histidine-tagged AgrD driven by P_{HELP}. Another vector was generated to drive expression of 6x-His-AgrD under the control of the P_{HELP} promoter derived from pIMAY. P_{HELP} is a constitutive promoter (55). P_{HELP} was isolated from pIMAY using PCR and the fragment was then joined with the sequence for either the N-terminal or C-terminal 6x-histidine-tagged AgrD by SOEing PCR. For the N-terminally tagged AgrD construct PCR was performed using pIMAY as a template with oligonucleotides P_{HELP}-*agrD*-SOE1-PstI and P_{HELP}-*6xHis-agrD*-SOE2 while the pOS1-P_{hrt}-*agrD*-6xHis was used as template for a PCR reaction with oligonucleotides P_{HELP}-*6xHis-agrD*-SOE3 and P_{HELP}-*6xHis-agrD*-SOE4-BamHI. The resultant amplicons were then spliced together by SOEing PCR using olignoculeotides P_{HELP}-*agrD*-SOE1-PstI and P_{HELP}-*6xHis-agrD*-SOE4-BamHI. Similarly, the C-terminal construct was generated by PCR using pIMAY as a template with oligonucleotides P_{HELP}-*agrD*-SOE1-PstI and P_{HELP}-*agrD-6xHis*-SOE2, while pOS1-P_{hrt}-*6xHis-agrD* was the template for a second PCR with oligonucleotides P_{HELP}-*agrD-6xHis*-SOE3 and P_{HELP}-*agrD-6xHis*-SOE4-BamHI. These fragments were then spliced together by SOEing PCR and cloned into pOS1 using the PstI and BamHI restriction sites.

Construction of 6x-histidine-tagged AgrD overexpression vectors. Additional overexpression plasmids were generated using the P_{sarA} promoter, a highly transcribed promoter linked to the *sod* ribosomal binding site, an optimal ribosome binding site for *S. aureus*. These plasmids were constructed using SOEing PCR in a similar manner to the pOS1-P_{HELP} constructs described above. For the N-terminal 6x-histidine-tagged AgrD,

P_{sarA}-sod_{RBS} was amplified using oligonucleotides P_{sarA}- sod_{RBS} -SOE1-PstI and P_{sara}- sod_{RBS} -*6xHis-agrD*-SOE2. pOS1-P_{hrt}-*6xHis-agrD* was used as template along with oligonucleotides P_{sara}- sod_{RBS} -*6xHis-agrD*-SOE3 and P_{sara}- sod_{RBS} -*6xHis-agrD*-SOE4-EcoRI. These amplicons were then spliced together using primers P_{sarA}- sod_{RBS} -SOE1-PstI and P_{sara}- sod_{RBS} -*6xHisagrD*-SOE4-EcoRI and the resultant product was cloned into pOS1 using the PstI and EcoRI restriction sites. This plasmid was then transformed into DH5α, electroporated into RN4220, and then electroporated into wild type, Δ*1984*, Δ*1984+1984*, and Δ*agr* as described above. The C-terminal 6x-histidine-tagged AgrD construct under the transcriptional control of P_{sarA} was generated in the same way. pOS1-P_{hrt}-*agrD-6xHis* was used as the agrD template in a PCR reaction with oligonucleotides P_{sara}- sod_{RBS} -*agrD-6xHis*-SOE3 and P_{sara}- sod_{RBS} -*agrD-6xHis*-SOE4-EcorI and P_{sarA} was amplified using primers P_{sarA}-sod_{RBS}-SOE1-PstI and P_{sara}- sod_{RBS} -*agrD-6xHis*-SOE2. Again, a SOEing PCR was performed to splice these amplicons together using primers P_{sarA}- sod_{RBS} -SOE1-PstI and P_{sara}- sod_{RBS} -*agrD-6xHis*-SOE4-EcorI. This product was cloned into pOS1 using the PstI and EcoRI restriction sites, transformed into DH5α, electroporated into RN4220, and then electroporated into wild type, Δ*1984*, Δ*1984+1984*, Δ*agr* and Δ*1984*Δ*agr* as described above. The strains containing pOS1-P_{sarA}- sod_{RBS} -*agrD-6xHis* are referred to as WT+C, Δ*1984+C,* Δ*1984+1984+C,* Δ*agr+C,* and Δ*1984*Δ*agr+C*.

Construction of N-terminal 6x-histidine-tagged AgrD with a linker region construct. Lastly, troubleshooting issues with the detection of N-terminal 6x-histidine-tagged AgrD led us to generate an expression vector that used pOS1-P_{sarA}- sod_{RBS} as a promoter, but we added a linker region between the 6x-histidine-tag and the N-terminal

end of *agrD*. For these purposes the 6x-histidine-tag, an S- tag, *agrD*, and c-myc were amplified from an *E. coli* AgrD expression strain. pOS1-P_{sarA}- sod_{RBS} -*agrD-6xHis* was used as a template for a PCR using oligonucleotides UNI- P_{sara}- sod_{RBS} -SOE1-PstI and P_{sara}- sod_{RBS} -*6xHis-Linker-agrD*-SOE2. pET-41b-*agrD* was used as a template for a PCR using oligonucleotides P_{sara}- sod_{RBS} -*6xHis-Linker-agrD*-SOE3 and P_{sara}- sod_{RBS} -*6xHis-Linker-agrD*-SOE4-EcorI. These amplicons were then used in a SOEing PCR with oligonucleotides UNI- P_{sara}- sod_{RBS} -SOE1-PstI and P_{sara}- sod_{RBS} -*6xHis-Linker-agrD*-SOE4-EcorI. The resulting product was then cloned into the multi-cloning site of pOS1 using the PstI and EcoRI restriction sites, transformed into DH5α, electroporated into RN4220, and then electroporated into wild type, Δ*1984*, Δ*1984+1984*, Δ*agr* and Δ*1984*Δ*agr* as described above. The strains containing pOS1-P_{sarA}- sod_{RBS} -*6xHis-linker-agrD* are referred to as WT+N, Δ*1984+N*, Δ*1984+1984+N*, Δ*agr+N*, and Δ*1984*Δ*agr+N*.

Whole cell lysate preparation.

5 mL of *S. aureus* strains were grown overnight at 37°C with shaking at 200 rpm. Overnight cultures were diluted 1:50 in 20 mL of fresh medium and allowed to replicate for an additional 8 hours at 37°C with shaking at 200 rpm. After 8 hours, the OD600 nm was measured and samples were centrifuged at 4200 rpm for 15 minutes. Supernatants were removed and the bacterial cell pellets were stored at -80°C until use. Pellets were thawed on ice and resuspended in 250 μL of sterile PBS, 250 μL of PBS supplemented with 1 M NaCl (Amresco), or 250 μL of PBS supplemented with 1 M NaCl and 6 M Urea (VWR). The resuspended bacteria were then added to screw cap microcentrifuge lysing tubes (Fisher Scientific) containing 250 μL 0.1 mm glass cell disruption beads

(Scientific Industries, Inc.). Cells were lysed using a Fast Prep-24 5G (MP Biomedicals). Cells were disrupted at speed 5.0 for 20 seconds, allowed to recover on ice for 5 minutes, and then disrupted a second time at speed 4.5 for 20 seconds. Samples were then either (a) centrifuged at maximum speed for 15 minutes at 4°C and 45 µL of supernatants were collected and boiled for 10 minutes with 15 µL of 6x SDS sample buffer (0.375 M Tris pH6.8, 12 SDS, 60% glycerol, 0.6 M DTT, 0.06% bromophenol blue), or (b) 50 µL of 6x SDS Sample buffer was added directly to lysed cells and boiled for 10 minutes. After boiling, the tubes were centrifuged at maximum speed for 15 minute at 4°C and supernatants were collected. These two preparations allowed for the collection of a soluble cell lysate fraction and total (soluble and insoluble) proteins. Samples were stored at -20°C for no longer then a few days.

Exoprotein preparations.

S. aureus strains were grown at 37°C with shaking at 200 rpm overnight. Overnight cultures were diluted 1:50 in fresh medium and allowed to grow 8 hours to stationary phase at 37°C with shaking at 200 rpm. After 8 hours, the OD600 nm was measured and samples were centrifuged at 4200 rpm for 15 minutes. 1.3 mL of supernatants were collected in 1.5 mL eppendorf tubes and cooled on ice for approximately 30 minutes. Next, 150 µl of 100% tri-chloro acetic acid (TCA) was added to the samples and the tubes were mixed by inversion followed by overnight incubation at 4°C. The next day samples were centrifuged at 4°C for 15 minutes at maximum speed and supernatants were removed and discarded. Samples were incubated in 1 mL of 100% ethanol (Decon Laboratories Inc.) for 30 minutes at 4°C followed by another 15 minute spin at 4°C at maximum speed. Supernatants were again discarded and pellets dried at

room temperature for about one hour. Pellets were then dissolved in TCA-SDS sample buffer (0.5 M Tris-HCL buffer, 4%SDS mixed 1:1 with 2x SDS Sample buffer) and boiled for 10 minutes before storage at -20°C.

Affinity-based enrichment of 6x-histidine-tagged AgrD.

S. aureus strains were grown at 37°C with shaking at 200 rpm overnight and then diluted 1:50 in fresh medium and let grow 8 hours at 37°C with shaking at 200 rpm. After 8 hours, the OD600 nm was measured and samples were centrifuged at 4200 rpm for 15 minutes. Supernatants were removed and the pellets (bacterial cells) were stored at -80°C. Pellets were thawed on ice and resuspended in 250µl sterile PBS supplemented with 1M NaCl and 1mM phenylmethanesulfonyl floride (PMSF) (Acros organics). The suspended bacteria were then added to screw cap microcentrifuge lysing tubes (Fisher Scientific) containing 250 µL 0.1 mm glass cell disruption beads (Scientific Industries, Inc.). Cells were lysed using a Fast Prep-24 5G (MP Biomedicals) by two disruption steps. First, cells were disrupted at speed 5.0 for 20 seconds and allowed to recover on ice for 5 minutes. Then cells were disrupted a second time at speed 4.5 for 20 seconds. Lysates were centrifuged at maximum speed for 15 minutes at 4°C. Supernatants were then incubated with Ni-NTA superflow nickel resin (Qiagen) for 1 hour at room temperature on a rotisserie. Following incubation, the resin was centrifuged at 3000 rpm for 3 min and supernatants were discarded. The resin was then washed six times in PBS with 1M NaCl and 25 mM Imidazol (Amresco). After the last wash, the resin was resuspended in 6x SDS buffer and boiled for 10 minutes followed by centrifugation at 3000 rpm for 3 minutes, removal of supernatant, and storage at -20°C.

Immunoblot for virulence factors.

Wild type, Δ*1984*, Δ*1984+1984*, and Δ*agr* strains were grown in 5 mL of RPMI for eight hours at 37°C with shaking at 200 rpm and supernatants were collected for TCA precipitation as described above. Once prepared, protein samples were normalized based on OD600nm and were separated by sodium dodecyl sulfate polyacrylamide gel electrophoresis (SDS-PAGE) in 12% polyacrylamide gels at 120 volts in a Quadra Mini-Vertical PAGE/Blotting System (CBS Scientific). Resolved proteins were then transferred from polyacrylamide gels to 0.45 μm PVDF membranes (Immobilon, Roche) at 200 V for 1 hr. After transfer, membranes were stored overnight in PBST (0.1% Tween -20 (Amresco) in PBS (Corning)) at 4°C. Membranes were then blocked in PBST with 1% Bovine Serum Albumin (BSA) (Amresco) for 1 hour while rocking. Following this blocking step, rabbit anti-LukA and rabbit anti-LukE antibodies (57), at a 1:7500 dilution in PBST supplemented with 1% BSA, were incubated with the membranes and allowed to rock for 1 hour. Although these antibodies recognize LukAB and LukED, we are also able to detect Protein A due to its binding of the F_C region of antibodies. Following incubation with the primary antibodies, membranes were washed three times in PBST for 15 minutes and goat anti-rabbit IgG (H+L) HRP conjugate (Thermo) was then added at a 1:400 dilution in PBST with 1% BSA for 1 hour while rocking. After this incubation the membranes were washed 3 more times in PBST for 15 minutes each and immunoblot images were captured on FluorChem System (Protein Simple) using SuperSignal West Pico Chemiluminiscent Substrate (Thermo).

Immunoblot of cleavage events.

Strains containing plasmids with either the C-terminal or N-terminal 6x-histidine-tagged *agrD* were grown in 20 mL of RPMI for eight hours at 37°C with shaking at 200 rpm and supernatants and cell lysates were processed as described above. Protein samples were either normalized to growth based on OD600nm or based on band intensity in prior immunoblots. Proteins were separated by sodium dodecyl sulfate polyacrylamide gel electrophoresis (SDS-PAGE) in 12% polyacrylamide gels at 120 volts in a Quadra Mini-Vertical PAGE/Blotting System (CBS Scientific) or by Tricine-SDS-PAGE (Schagger 2006) in 21% polyacrylamide gels with 6M urea at 200 to 300 volts in a Hoefer™ SE 600 series electrophoresis apparatus. Resolved proteins were then transferred from polyacrylamide gels to 0.20 μm PVDF membranes (Immobilon, Roche) at 70 V for 75 minutes in a Quadra Mini-Vertical PAGE/Blotting System (CBS Scientific). Immediately following transfer, membranes were fixed in a 4% paraformaldhyde (Alfa Aesar) solution for 30 minutes at room temperature. Membranes were then washed for 20minutes in PBST and blocked overnight in PBST with 5% Milk (Roundy's) at 4°C with rocking. The next day the membranes were washed in PBST 3 times for 20 minutes. Mouse anti-6x-histidine antibody (Abcam) at a 1:3000 dilution in PBST with 1% BSA was incubated with each membrane for 1 hour at room temperature followed by three 20 minute washes with PBST. Secondary goat anti-mouse IgG (H+L) HRP conjugate (Thermo) was then added at a 1:400 dilution in PBST with 1% BSA for 1 hour while rocking followed by four washes for 20 minutes each in PBST. Immunoblot images were captured on BioDot blue autoradiography film (Dot Scientific) using SuperSignal West Pico Chemiluminiscent Substrate (Thermo).

Membrane Fraction preparation and application of purified AgrD.

Strains containing the C-terminal 6x-histidine-tagged AgrD were grown overnight in TSB at 37°C with shaking at 200 rpm. The next morning cultures were diluted 1:100 in 50 mL of fresh medium and grown for 6 hours at 37°C with shaking at 200 rpm. Samples were then centrifuged at max speed for 15 minutes, the supernatants were discarded and the bacterial pellets stored at -80°C overnight. The next day, the pellets were thawed on ice before being resuspended in 4 mL of Birnboim solution 1 (50mM glucose, 10 mM EDTA, 25 mM Tris-HCl (pH 8.0)) and 200µl of lysostaphin. Samples were incubated for at least 30 minutes at 37°C with shaking at 200 rpm. After incubation, cells appeared lysed and samples were cooled to approximately 4°C on ice. Once cooled, samples underwent 3 rounds of sonication for 30 seconds each at 20% power with 5 minutes of cooling on ice between rounds of sonication. Following sonication, samples went through 3 freeze thaw cycles in a dry ice-ethanol bath and one additional round of sonication. Intact cells were then removed with a low speed centrifugation at 500 g for 3 min at 4°C. Supernatants were collected and placed in thick-walled microfuge tubes and centrifuged at 50,000 g for 45 minutes at 4°C. After centrifugation, the supernatant containing the soluble fraction was discarded and the pellet containing the membrane fraction was resuspended in 300 µl of membrane extraction buffer (50mM HEPES (pH 7.4), 125mM NaCl, 5% v/v glycerol, and 1% (W/W) dodecyl maltoside (DDM)). Samples were then moved to new conical tubes and underwent a final 2 rounds of sonication for 1 second each at 10% power using a microprobe. Samples containing *S. aureus* membranes were placed on a rocker at 4°C for 1 hour and then aliquoted and stored at -20°C.

Alex Argianas purified 6x-histidine-tagged AgrD using affinity purification and Fast Protein Liquid Chromatography (FPLC), and samples were stored at -20°C. Membrane fractions as well as purified AgrD were thawed on ice and protein levels were measured using Pierce™ BCA Protein Assay Kit (Thermo Scientific). 50 μg of membrane proteins were incubated with 1-3 μl of purified AgrD at 25°C for 90 minutes. After incubation, 60 μl of 2x SDS buffer was added to each reaction and boiled for 10 minutes. Proteins were then separated by SDS-PAGE electrophoresis and transferred to a 0.2 μm PVDF membranes, and immunodetection of cleavage events was performed as previously described.

Mass spectrometry.

Exoprotein preparations of wild type, Δ*1984*, Δ*1984+1984,* and Δ*agr* strains were collected as described above. Once prepared, protein samples were normalized based on OD600nm and were separated by sodium dodecyl sulfate polyacrylamide gel electrophoresis (SDS-PAGE) in 12% polyacrylamide gels at 120 volts in a Quadra Mini-Vertical PAGE/Blotting System (CBS Scientific). All equipment was washed with 4% sodium dodecyl sulfate (SDS), deionized water, and ethanol before use and fresh buffer was used. Gels were stained with coomassie blue, bands cut out with a cleaned razor blade, and gel slices placed in snap closure tubes before being submitted for Mass spectrometry (Alphalyse Pick n' Post).

Macrophage cytokine Profiles.

Bacteria were grown overnight in triplicate in a 96-well round bottom plate (Corning) in 150 μl of TSB at 37°C with shaking at 200 rpm. Samples were then diluted in a 96-well round bottom plate 1:50 in 147 μl of fresh TSB and incubated for 8 hours at

37°C with shaking at 200 rpm. Bacterial growth was assessed by reading the optical density at 600 nm followed by centrifugation at 3700 rpm for 15 minutes. Supernatants were collected and stored at -80°C. Primary bone marrow derived macrophages (BMDM) were thawed and incubated at 37°C with 5% CO_2 for 48 hours before seeding in a 96 well plate at 65,000 cells per well. BMDM were allowed to rest overnight before being treated with 10 µl of bacterial supernatant for 24 hours at 37°C at 5% CO_2. After 24 hours 50 µl of supernatants were collected and stored at -80°C. To assess cytokine levels, a BD™ Cytometric Bead Array Mouse Soluble Protein Set and Soluble Protein Master Buffer Kit were used. The manufacturer's instructions were followed except each well contained 0.1 µl of each bead and 0.1 µl of each detection reagent for ten different cytokines.

AIP reporter assay.

Wild type, Δ*1984*, and Δ*agr* strains containing pDB59 (described above) as well as Δ*1984+1984* were cultured overnight in TSB supplemented with Cm at 37°C with shaking at 200 rpm. The next day samples were diluted 1:100 in fresh TSB and incubated for 5 hours at 37°C with shaking at 200 rpm. Samples were centrifuged at 4,200 rpm for 10 minutes. Supernatants were collected and filter sterilized through a 0.45 nm syringe filter and diluted 1:1 in fresh TSB. The pellets were then resuspended in 5 mL of the conditioned medium and incubated an additional two hours. After this incubation, the bacteria were washed in PBS twice and resuspended in 1mL of PBS. Samples were then diluted two fold in PBS and aliquoted in triplicate into a flat bottom 96 well plate. Bacterial optical density (OD600) as well as GFP levels (EX 395 nm, EM 509 nm), were measured using an Omega plate reader. The data were normalized and displayed as GFP/OD.

Murine Infection models.

All animal experiments in this study were performed in an ABSL2 facility with protocols approved by Loyola University of Chicago following the standards set forth by the Institutional Animal Care and use Committee. For this study, 6 to 8 week old female Swiss Webster mice (Envigo) were used and monitored daily after infection. Each experiment contained cohorts of at least 4 mice and was repeated at least 3 times.

Murine Peritonitis infections. Cultures of wild type, Δ*1984*, Δ*1984+1984*, and Δ*agr* were inoculated from freshly isolated single colonies and grown with shaking at 37°C overnight. The next day, a 1:100 subculture into 15 mL of TSB was incubated at 37°C for 3 hours with shaking at 200 rpm. After incubation, cultures were then centrifuged for 5 minutes at maximum speed and cell pellets were washed twice in 5 mL of PBS. Once washed and resuspended in 5 mL of PBS, bacterial suspensions were then normalized to an O.D. of approximately 1.1 (1×10^9 CFU/mL). Mice were infected intraperitoneally with ~1×10^8 CFU of bacteria in 100 µl of PBS. Mice were monitored daily and at approximately 72 hours post-infection were euthanized followed by peritoneal lavage and isolation of kidneys. Tissues were aseptically isolated, homogenized, spread onto TSA plates, and incubated overnight at 37°C in order to enumerate CFU. Serum was also collected from each infected animal. Serum and peritoneal lavage samples were then used for cytometric bead array to examine cytokine levels as previously described. Immune cell populations were isolated from the kidney, spleen, and peritoneal lavage and analyzed by flow cytometry for known markers of phagocytic and lymphocytic cell populations and their activation status. For phagocytic cell populations I used CD11b, Ly6G, CD11c, Dx5, CD14, CD206, IA/IE, and F4/80

markers while I used CD44, CD11b, CD8, CD3, NK1.1, TCRγ/δ, CD4, and B220 for lymphocyte populations.

Murine systemic infections. Cultures of wild type, Δ*1984*, Δ*1984+1984*, and Δ*agr* were inoculated from freshly isolated single colonies and grown with shaking at 37°C overnight. The next day, a 1:100 subculture into 15 mL of TSB was incubated at 37°C for 3 hours with shaking at 200 rpm. After incubation, cultures were then centrifuged for 5 minutes at maximum speed and cell pellets were washed twice in 5 mL PBS. Once washed and resuspended in 5 mL of PBS, bacterial suspensions were diluted 2mL into 8 mL of PBS and normalized to an O.D. of approximately 0.32-0.33 (1×10^8 CFU/mL). Mice were first deeply anesthetized with 2,2,2- tribromoethanol (Avertin; Sigma) via intraperitoneal injection and then inoculated with 100 µl PBS containing $1x10^7$ CFU of bacteria into the bloodstream via the retro-orbital venous plexus. Mice were monitored daily until 96 hours post-infection, at which point they were euthanized and kidney, heart, and liver were harvested. Tissues were aseptically isolated, homogenized and spread onto TSA plates and incubated overnight at 37°C in order to enumerate CFU. Additionally, serum was collected and immune cells were isolated for flow cytometry analysis of immune cell recruitment as described above.

Murine skin and soft tissue infections. Cultures of wild type, Δ*1984*, Δ*1984+1984*, and Δ*agr* were inoculated from freshly isolated single colonies and grown with shaking at 200 rpm at 37°C overnight. The next day, a 1:100 subculture in 15 mL of TSB was incubated at 37°C for 3 hours with shaking. After incubation, cultures were then centrifuged for 5 minutes at maximum speed and cell pellets were washed twice in 5 of mL PBS. Once washed and resuspended in 5 mL of PBS, bacterial suspensions were

diluted 2mL into 8 mL of PBS and normalized with PBS to reach to an O.D. of approximately 0.32-0.33 (1 x 10^8 CFU/mL) and mixed 1:1 with sterile Cytodex beads (Sigma). Mice were first deeply anesthetized with 2,2,2- tribromoethanol (Avertin; Sigma) via intraperitoneal injection. After anesthetization, mice flanks were shaved and inoculated with 100 μl PBS containing 1x10^7 CFU of bacteria and Cytodex beads on the right and left side by intradermal injection. Mice were monitored daily and at 72 or 120 hours post-infection mice were euthanized. Skin abscesses were collected, homogenized, spread onto TSA plates, and incubated overnight at 37°C in order to enumerate CFU. Skin homogenates and serum were also collected for cytometric bead array analysis for cytokine levels, as previously described.

CHAPTER THREE

EXPERIMENTAL RESULTS

Determine whether the function of 1984 is linked to Agr activity

Introduction. Over the past several decades, cases of both hospital-acquired and community-acquired *S. aureus* infections have increased, resulting in over 300,000 hospitalizations and 11,000 deaths a year (2, 3). This rise in infection rates is thought to be due to both increased incidence of antibiotic resistance among infectious isolates as well as alterations in virulence factor gene expression, allowing more efficient immune evasion. *S. aureus* uses complex and redundant regulatory systems to produce a diverse array of cytotoxins and virulence factors that promote its survival. These same virulence factor regulatory schemes allow *S. aureus* to evade the complex innate immune surveillance mechanisms it encounters. For these reasons, it is important to understand the mechanisms used by *S. aureus* to control virulence factor gene expression and promote its pathogenesis.

Previous identification of a *1984* mutant during a transposon mutant library screen. Deciphering the mechanisms that *S. aureus* uses to interact with cells of the immune system will help us to understand how *S. aureus* evades critical host defense strategies. To identify factors that positively or negatively modulate macrophage activity, Dr. Alonzo conducted a screen using supernatants derived from an annotated transposon mutant library of *S. aureus*. These supernatants were applied to murine bone marrow

derived macrophages and cytokine production was examined by cytometric bead array. Mutants were identified that either positively or negatively altered cytokine production to a significant degree. One mutant that elicited a hyper-inflammatory macrophage response contained a transposon insertion in the gene *SAUSA300_1984.* This mutant induced the production of IL-1β at levels greater than two standard deviations from the mean induced by all other mutants in the screen (Figure 3). Because only cell free supernatant was applied to the macrophages, Dr. Alonzo hypothesized that the secreted factors from *1984::erm* might be different from wild type *S. aureus*. Consistent with this hypothesis, Dr. Alonzo has shown that *1984::erm* does have an altered exoprotein profile that lacks many proteins present in wild type supernatant (Figure 4). To begin to determine whether 1984 plays a role in pathogenesis, Dr. Alonzo used the *1984::erm* transposon mutant in a murine peritonitis model of infection. Dr. Alonzo enumerated the bacterial colony forming units (CFUs) at three sites: the kidney, peritoneal cavity, and blood after 16 hours of infection (Figure 5). He found that the bacterial burden of *1984::erm* was lower than that of wild type *S. aureus* in each site (Figure 5). These data suggested that the function of 1984 is critical for *S. aureus* survival during infection and supported further study of the function of 1984.

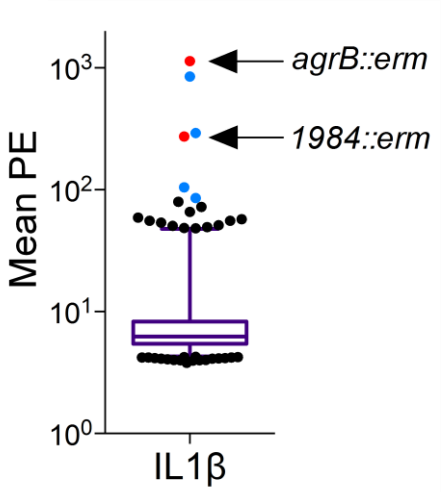

Figure 3. A *1984::erm* transposon mutant elicits an enhanced IL-1β response in macrophages. Murine bone marrow derived macrophages were incubated with supernatants derived from an *S. aureus* transposon mutant library and IL-1β cytokine production levels were measured. Blue circles represent mutants that elicited cytokine production by the macrophages greater than two standard deviations from the mean induced by all other mutants. Pink circles represent *1984::erm* and *agrB::erm*, respectively. Courtesy of Dr. Alonzo.

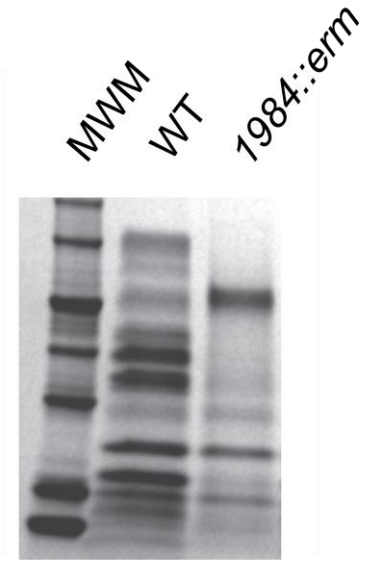

Figure 4. Exoprotein profile of a mutant with a transposon insertion in *1984* is altered compared to that of wild type *S. aureus.* Wild type and *1984::erm* were grown in TSB for 9 hours at 37°C with shaking at 200 rpm before supernatants were collected, processed, and resolved by SDS-PAGE. Gel stained with coomassie. Courtesy of Dr. Alonzo.

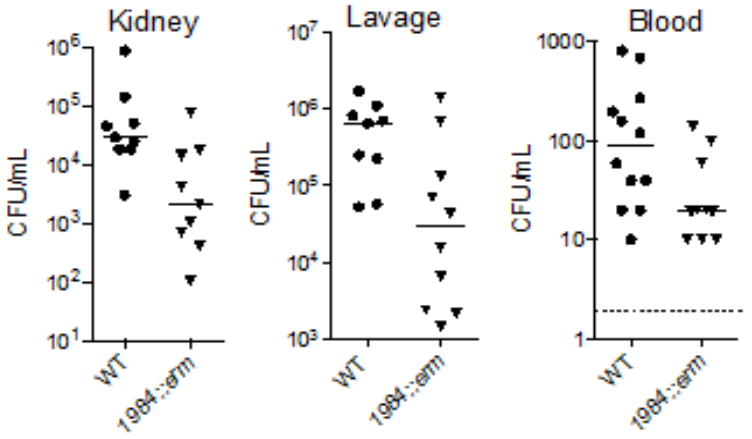

Figure 5. A *1984::erm* mutant is attenuated *in vivo.* Mice were infected with 1x10^8 CFU of wild type *S. aureus* or the transposon mutant using a peritoneal infection model and CFU were enumerated 16 hours post infection in kidney, peritoneal lavage, and serum. Courtesy of Dr. Alonzo.

A Δ*1984* mutant phenotypically mimics a Δ*agr* mutant. During the transposon mutant screen, phenotypic similarities between transposon insertions in *1984* and *agrB* were observed. The similarities between these two mutants included major defects in bacterial protein secretion and increased IL-1β secretion by macrophages (Figure 3). The Agr system is a major regulatory system in *S. aureus* that is involved in surface protein expression as well as virulence factor production and it contributes to the pathogenesis of *S. aureus* during infection. Based upon the influence of the Agr system on pathogenesis and the similarities between the transposon insertion mutants of *1984* and *agrB*, I decided to investigate similarities between in-frame deletion mutants of *1984* and *agr*, and compared their protein secretion profiles, virulence factor production, ability to induce macrophage activation, and pathogenesis *in vivo*. As a *1984* transposon insertion mutant displayed similar phenotypes to a transposon insertion mutant in *agrB*, I hypothesized that a Δ*1984* mutant would display similar phenotypic markers associated with Agr deficiency such as reduction in secreted proteins, decreased virulence factor expression,

increased surface protein expression, and altered macrophage activation compared to wild type *S. aureus*. Consistent with the findings of the transposon mutants, I found that a Δ*1984* mutant phenocopies a Δ*agr* mutant for defects in protein secretion in both rich and defined media (Figure 6).

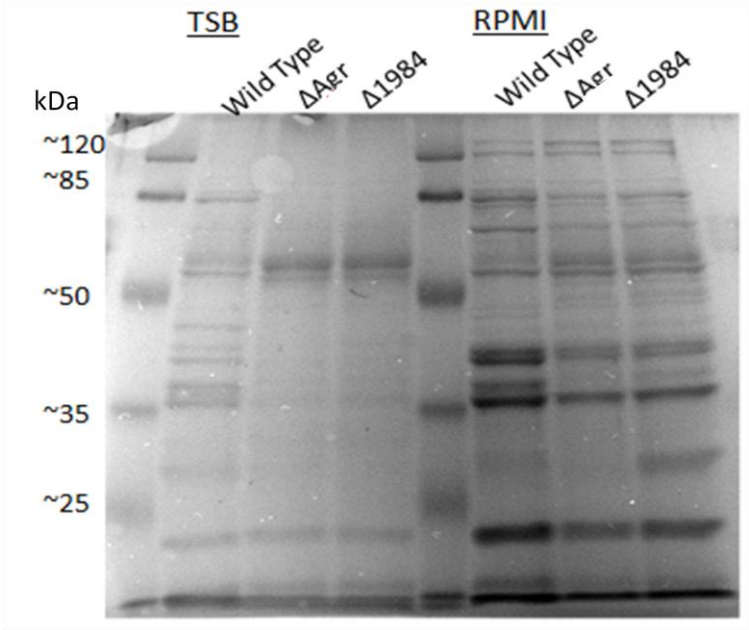

Figure 6. A Δ*1984* mutant resembles a Δ*agr* mutant for defects in protein secretion. Exoprotein profiles from wild type, a Δ*1984* mutant, and a Δ*agr* mutant grown in rich (TSB) and defined (RPMI) medium for eight hours.

To verify results seen during the transposon mutant screen as well as to compare the roles of 1984 and the Agr system in macrophage activation, I repeated the above-described macrophage cytokine assay with a Δ*1984* mutant. If a Δ*1984* mutant were defective in protein secretion similar to a Δ*agr* mutant, then I would expect to see a similar pro-inflammatory cytokine response when bone marrow derived macrophages are treated with supernatant from a Δ*1984* mutant and a Δ*agr* mutant. I found that supernatant from a Δ*1984* mutant and a Δ*agr* mutant altered macrophage cytokine secretion in a similar manner. The supernatants of both strains induced significantly higher levels of IL-1β secretion, but led to decreases in the levels of IL6 and KC

compared to supernatant from wild type or Δ*1984+1984* strains (Figure 7). The similarities in cytokine secretion profiles after treatment of macrophages with supernatant derived from Δ*1984* and Δ*agr* mutants provided the first evidence that the functions of *1984* and *agr* might converge, leading to similar in vitro and in vivo phenotypes.

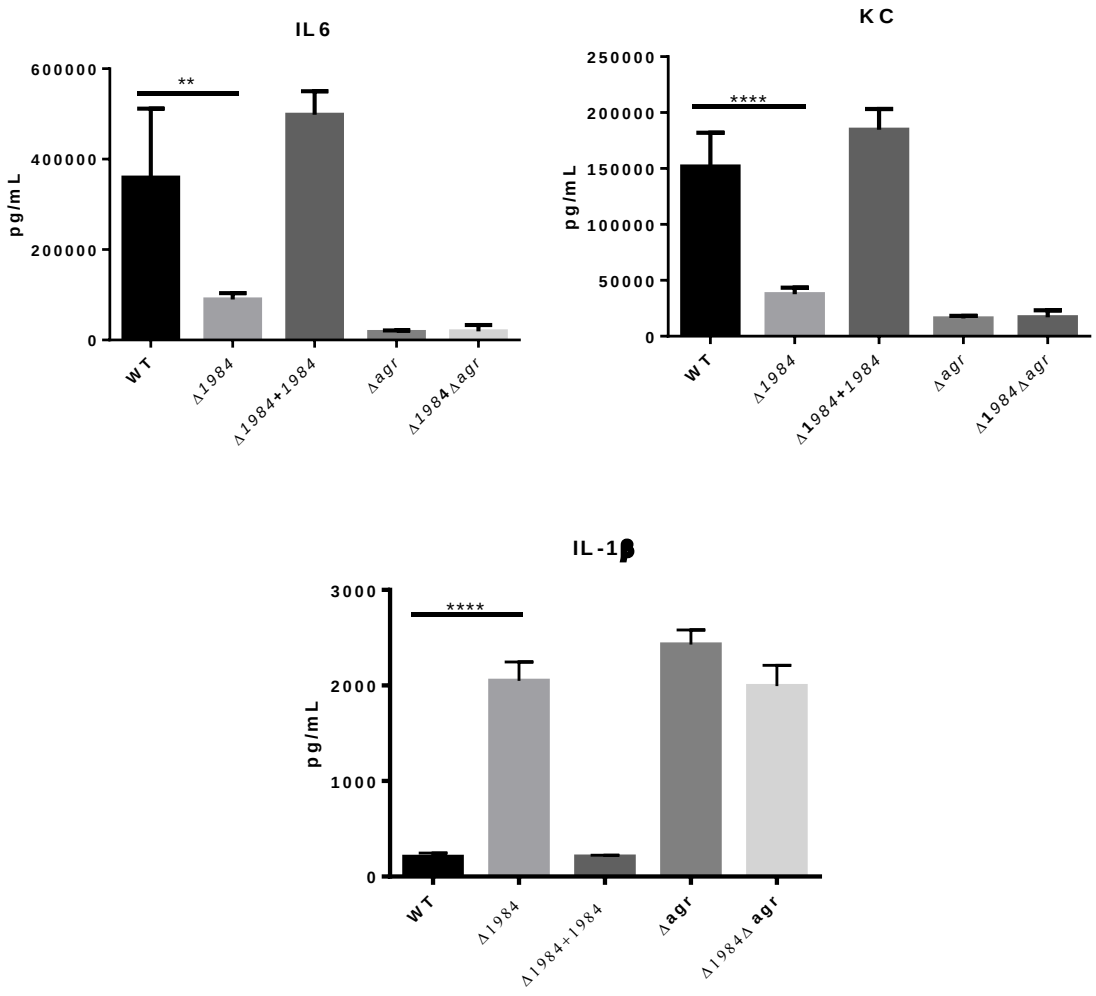

Figure 7. A Δ*1984* mutant phenocopies a Δ*agr* mutant for macrophage immunomodulation. Murine bone marrow derived macrophages were incubated with cell free supernatant from wild type *S. aureus,* Δ*1984*, Δ*1984+1984*, Δ*agr*, and Δ*1984*Δ*agr* for 24 hours. CBA was performed on macrophage supernatant. Data shown are a representative experiment with triplicate values. A one-way ANOVA was used to evaluate the significance of the data.

Based on the similarities between exoprotein profiles and macrophage activation between a Δ*1984* and a Δ*agr* mutant, we would expect other well-known regulatory

patterns associated with Agr deficiency to also be the same. The Agr pathway is involved in regulating virulence factors such as Protein A and leukotoxins in an opposing manner such that Protein A expression is decreased and leukotoxin expression is increased upon induction of the Agr pathway. Therefore, I evaluated Protein A and leukotoxin protein expression levels in a Δ*1984* mutant. Because a Δ*agr* mutant cannot induce production of RNAIII to elicit its regulatory functions, a Δ*agr* mutant has increased expression of Protein A, but decreased expression of leukotoxins such as LukAB and LukED. If the hypothesis that Δ*1984* phenocopies Δ*agr* is correct, we would expect a Δ*1984* mutant to also have increased Protein A and decreased LukAB and LukED compared to a wild type strain. This hypothesis was tested by comparing virulence factor expression by immunoblots. Protein A levels were increased in both Δ*1984* and Δ*agr* compared to the wild type or the Δ*1984 +1984* complement strain. In contrast, the leukotoxin levels were decreased in a Δ*1984* mutant and a Δ*agr* mutant (Figure 8). Another secreted factor whose expression is positively regulated by the Agr system is the alpha toxin, the primary red blood cell lysing toxin of *S. aureus*. Therefore, a Δ*agr* mutant exhibits decreased hemolytic activity when on a blood agar plate compared to wild type *S. aureus* (Data not shown). Similarly, a Δ*1984* mutant is ineffective at creating a zone of clearance compared to wild type or Δ*1984+1984* (Figure 9). Together, these data provide clear evidence that a Δ*1984* mutant behaves similarly to a Δ*agr* mutant.

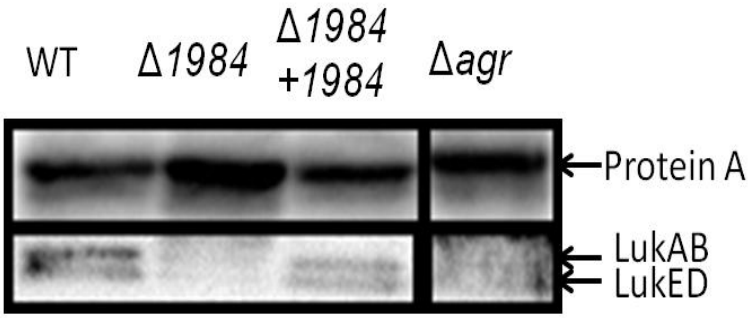

Figure 8. A Δ*1984* mutant phenocopies a Δ*agr* mutant for increases in Protein A expression and decreases in leukotoxin expression. Immunolots were performed on supernatant samples collected after 8 hours of growth. A rabbit anti-LukA antibody and a rabbit anti-LukE antibody were used for immunodetection.

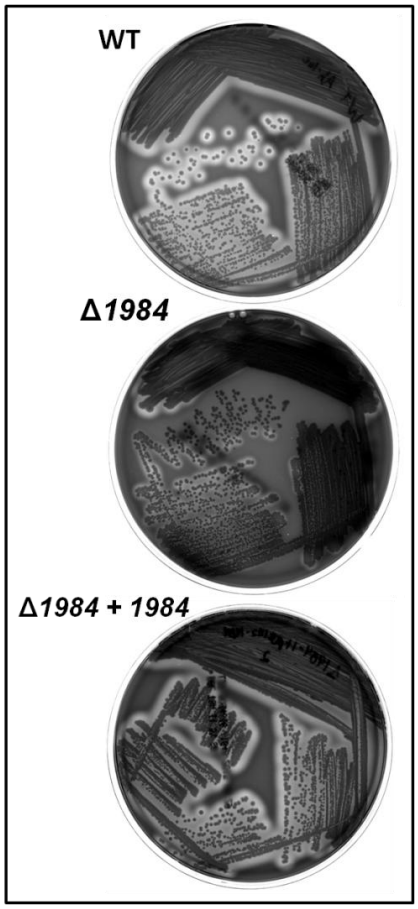

Figure 9. A Δ*1984* mutant has decreased hemolysis compared to wild type *S. aureus.* Strains were struck on a blood agar plate and grown at 37°C overnight.

Assess whether 1984 is involved in processing AgrD and generating functional AIP.

Introduction. Since a Δ*1984* mutant phenocopies a Δ*agr* mutant for exoprotein profile defects, alterations in virulence factor production, and macrophage activation, we hypothesized that 1984 may have a functional role in Agr system activation. As previously described, the Agr quorum-sensing system is comprised of a response regulator, AgrA, a histidine kinase, AgrC, the AIP peptide precursor, AgrD, and a transmembrane protein, AgrB (Figure 1A). The current literature indicates that AgrB is involved in AgrD post-translational processing by cleaving the C-terminal end of the peptide (48) as well as secreting processed AIP (9)(Figure 1B). In addition, Kavanaugh *et. al.* put forward the hypothesis that the Type I Signal Peptidase, SpsB, is responsible for cleaving the N-terminus of AgrD, however a number of weaknesses in the study design suggest that SpsB is an unlikely candidate for peptide processing (See Literature Review) (23). Therefore, the enzyme involved in cleaving the AgrD N-terminus remains unknown. Given this information along with my preliminary data, I hypothesized that 1984 is the peptidase responsible for cleaving the N-terminal end of AgrD. If this hypothesis were true, then a Δ*1984* mutant would not be expected to produce functional AIP, thereby rendering the Agr system inactive.

AIP production is compromised in a Δ*1984* mutant. My preliminary data show that a Δ*1984* mutant functionally mimics a Δ*agr* mutant, suggesting that 1984 is important for Agr system activation. To test whether or not 1984 facilitates AIP processing, I first determined if a Δ*1984* mutant is able to produce active AIP, with the expectation that if 1984 is involved in AgrD peptide processing then a Δ*1984* mutant would either not secrete AIP at all or would release a non-functional processing

intermediate. The presence or absence of active AIP can be measured by applying filtered culture supernatants to an AIP-responsive reporter strain. I used a Δ*1984* mutant, as well as a Δ*agr* mutant, that contained a reporter plasmid, pDB59, which contains the *P3* promoter from the Agr system controlling *gfp* transcription. Addition of supernatant that contains functional AIP will induce the *P3* promoter, leading to the production of GFP that can be measured with a fluorescence plate reader. In contrast, supernatant that lacks functional AIP, such as supernatant derived from a Δ*agr* mutant, will fail to induce high levels of GFP. As expected, the control Δ*agr* + pDB59 mutant does not produce GFP even in the presence of supernatant with fully processed AIP, which is consistent with the lack of AgrA and AgrC in this mutant (Figure 10). Additionally, supernatants from wild type *S. aureus* or Δ*1984*+*1984* both induced GFP production by Δ*1984*+pDB59, while supernatant derived from a Δ*agr* mutant failed to induce GFP production. Finally, I asked if supernatant derived from a Δ*1984* mutant can induce *P3* promoter activity, and found that Δ*1984* supernatant did not induce GFP production. From these results I can conclude that a Δ*1984* mutant does not produce properly processed AIP and that the Agr pathway is defective at the level of AIP production since activity can be fully restored by adding processed AgrD to a Δ*1984*+pDB59 reporter strain.

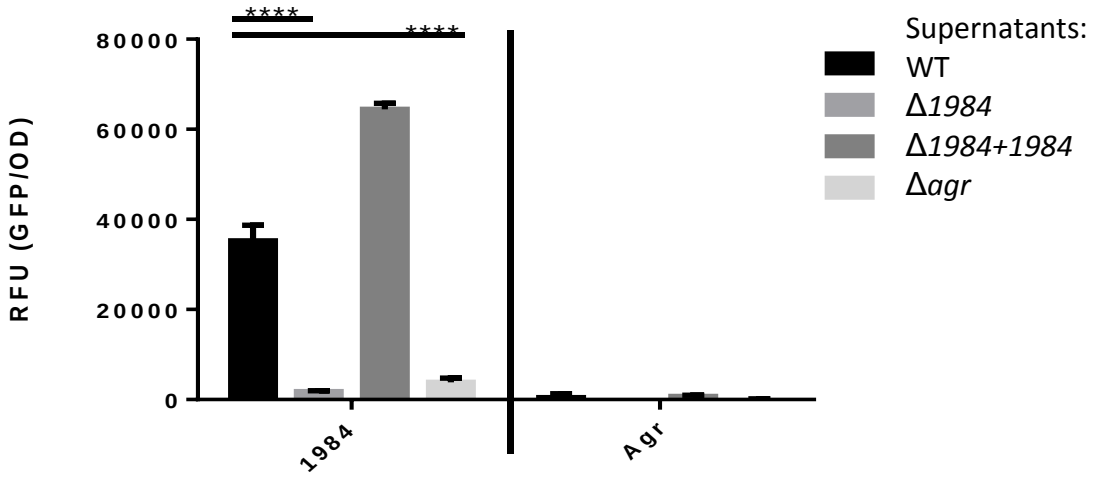

Figure 10. A Δ*1984* mutant does not produce functional AIP. A Δ*1984* mutant and a Δ*agr* mutant containing a pDB59 plasmid with the *P3* promoter of the Agr system promoting the expression of GFP was incubated with cell free supernatant from wild type, Δ*1984*, Δ*1984+1984*, and Δ*agr*. In the presence of properly processed AIP, in a genetic background containing AgrA and AgrC, *gfp* expression is induced. Statistical analyses were done using two-way ANOVA. **** P<0.0001.

Designing 6x-His-AgrD expression plasmids to evaluate 1984-dependent peptide processing.

(1) Native promoter expression. My *P3-gfp* reporter assays demonstrated that a Δ*1984* mutant cannot produce functional AIP as evidenced by a lack of promoter activity in the presence of conditioned medium derived from a Δ*1984* mutant. Furthermore, 1984 has predicted peptidase activity based on bioinformatics analysis. Given this information, I hypothesized that 1984 is involved in cleaving the N-terminal end of AgrD to generate functional AIP. To test this hypothesis I sought to visualize AgrD cleavage events by immunoblot, similar to those used to investigate the involvement of AgrB in C-terminal AgrD cleavage (11, 12, 58). If 1984 is involved in AgrD cleavage, then I should be able to visualize alterations in peptide lengths in the presence and absence of 1984 by

evaluating shifts in the molecular weight of 6x-His-tagged peptide fragments after immunoblotting with monoclonal anti-6xHis antibody as illustrated in Figure 11.

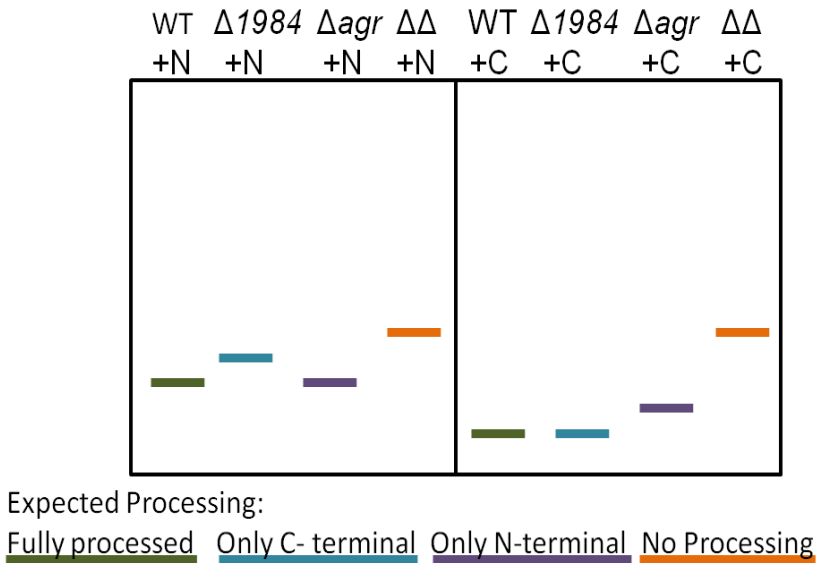

Figure 11. Expected results of AgrD cleavage. Wild type, a Δ*1984* mutant, a Δ*agr* mutant, as well as Δ*1984*Δ*agr* double mutant strains containing AgrD with a 6x-His-tag on either the C-terminal end or N-terminal end of the peptide should display varying AgrD processing intermediates.

In order to visualize alterations in peptide lengths in the presence or absence of 1984, I first needed to express 6x-His-tagged AgrD in wild type, Δ*1984*, Δ*agr*, and Δ*1984*Δ*agr* strains. Under normal conditions, the expression of AgrD peptide is driven by a promoter known as *P2*. *P2* promoter activity is sufficient to generate enough AIP to activate the Agr system in culture and is presumably detectable by immunoblot. Therefore, I first generated two native promoter AgrD expression vectors that kept expression of AgrD under the regulation of its native *P2* promoter. These two constructs encoded AgrB and either a C-terminal 6x-His-tagged AgrD or an N-terminal 6x-His-tagged AgrD (Figure 12A). Of note, inherent in use of the native promoter constructs is *agrB*, which precludes assessment of peptide cleavage events independent of the AgrB

protease even in Δ*agr*, and Δ*1984*Δ*agr* strain backgrounds. After growing strains containing these 6x-His-AgrD promoter constructs in RPMI medium for 8 hours, followed by collection of supernatant and whole cell lysates, I determined that I was not able to detect 6x-His-AgrD or AgrD-6x-His using either of the native promoter expression strains (data not shown). The lack of detection in this study suggests that the concentration of AgrD expressed from its native promoter is insufficient to permit detection of the peptide by immunoblot, therefore alternate expression strategies may be more adequate and should be tested.

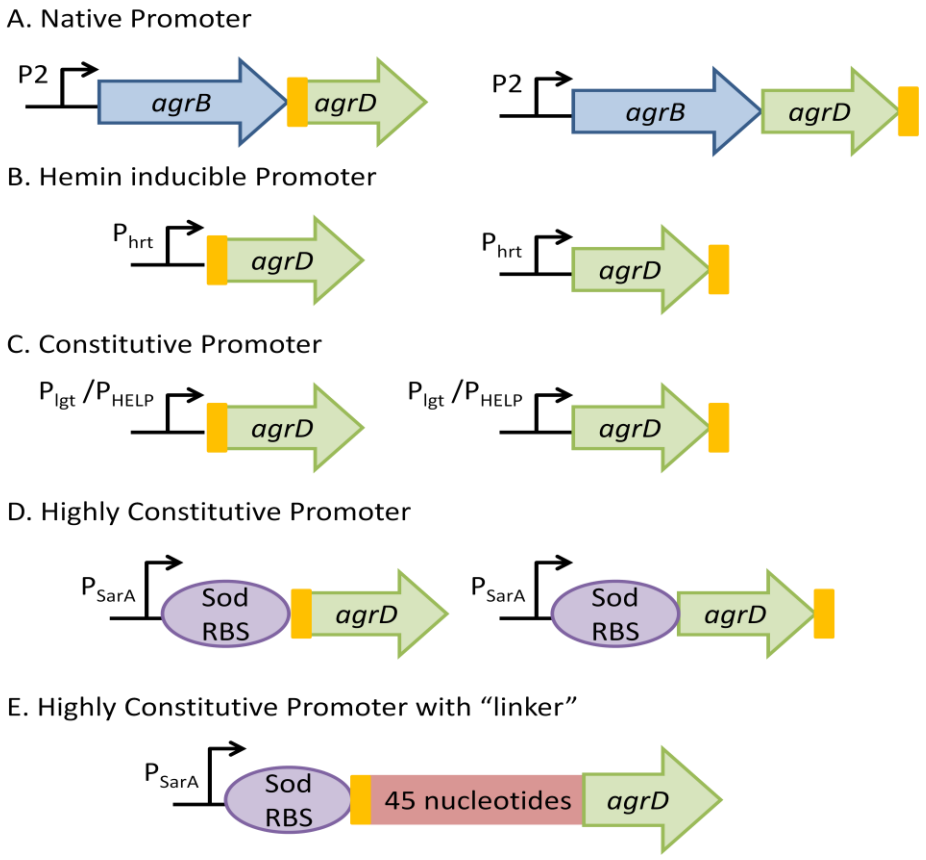

Figure 12. Illustration of 6x-histidine-tagged AgrD constructs. Expression plasmids were generated to drive AgrD expression under the control of: (A) its native *P2* promoter, (B) a hemin inducible promoter P_{hrt} , (C) constitutive promoters P_{lgt} and P_{HELP} and (D and E) the highly transcribed promoter, P_{SarA}, containing an optimal ribosomal binding. In order to troubleshoot issues with detection of the N-terminal 6x-histidine-tagged AgrD an S-tag was used as a linker region between the 6x-histidine-tag and AgrD in E. The yellow box represents the location of the 6x-histidine-tag.

(2) Hemin-inducible expression. It was clear from native promoter 6x-His-AgrD expression studies that AgrD was produced in insufficient quantities to permit visualization of peptide cleavage by immunoblot. Further, the presence of *agrB* in our native promoter expression constructs precluded our direct assessment of AgrB-independent cleavage. One method commonly used to enhance expression of target genes for downstream analysis is to drive expression under an inducible promoter. A number of *S. aureus* specific inducible promoters have been used including the hemin-inducible promoter P_{hrt}. Therefore, I sought to improve detection of 6x-His-AgrD by generating expression plasmids with either the N-terminal or C-terminal 6x-His-AgrD under the control of the P_{hrt} promoter (Figure 12B). With this expression vector I expected to induce a high level of 6x-His-AgrD upon addition of hemin that would be easily detected by immunoblot. After induction with concentrations of hemin that are not bactericidal and subsequent immunoblot, I still was unable to detect 6x-His-AgrD. Increased hemin concentrations that promote gene expression further were compromised by secondary toxic effects associated with adding excess hemin (data not shown). Together, these observations indicate that use of hemin-inducible promoter, P_{hrt}, is insufficient to permit high level expression and immunodetection of AgrD.

(3) Constitutive promoter expression. The hemin-inducible promoter P_{hrt} did not elicit high enough expression for immunodetection of AgrD without imposing significant cytotoxic effects. As an alternative approach to using this inducible expression plasmid, I sought to obtain detectable concentrations of 6x-His-AgrD using constitutive promoters in a multi-copy plasmid to drive 6x-His-AgrD expression. Two promoters commonly used in the *S. aureus* research community for constitutive expression are the

lipoprotein diacylglycerol transferase (P_{lgt}) promoter and the high expression in *Listeria* promoter (P_{HELP}). Therefore, to drive expression of 6x-His-AgrD, I created pOS1 expression plasmids with either P_{lgt} or P_{HELP} promoters driving *agrD* gene expression (Figure 12C). I expected these constructs to produce a large enough abundance of 6x-His-tagged AgrD to be detected by immunoblot, however none of these constructs led to detectable 6x-His-AgrD (data not shown). In sum, these studies indicated that, although 6x-His-tagged AgrD expression was under the control of constitutively expressed promoters, it is not expressed at high enough concentration for immunodetection.

(4) Use of high level overexpression vectors. 6x-His-tagged AgrD is undetectable by immunoblot even when constitutively expressed from the P_{lgt} or P_{HELP} promoters. This was surprising, given the routine use of these promoters to express genes in *S. aureus*. However, given this finding I needed to devise an alternative method to express 6x-His-AgrD. An additional highly expressed promoter that is routinely used to overexpress proteins in *S. aureus* is P_{sarA}. This particular *sarA* promoter is one of three promoters used by *S. aureus* to control the expression of the Staphylococcal accessory regulator (SarA). P_{sarA} is highly expressed in *S. aureus* and does not appear to be under additional regulatory control. Therefore, to attempt to achieve a detectable amount of 6x-His-tagged AgrD for immunoblot, I generated constructs using a multi-copy plasmid, pOS1, containing the P_{sarA} promoter and an optimized ribosomal binding site derived from the superoxide disumutase (*sod)* gene in *S. aureus* (Figure 12D). By over expressing the 6x-His-AgrD constructs I would expect to produce a high enough concentration of 6x-His-tagged AgrD to be detectable by immunoblot. Using this overexpression plasmid, I was finally able to detect the C-terminal 6x-His-tagged AgrD in whole cell lysates and

supernatant however I was still unable to detect the N-terminal 6x-His-AgrD (Figure 13). Together these data indicate that generation of sufficient quantities of ArgD for immunodetection requires significant overexpression from *S. aureus* and suggests that N-terminal 6x-His-AgrD may not be stable.

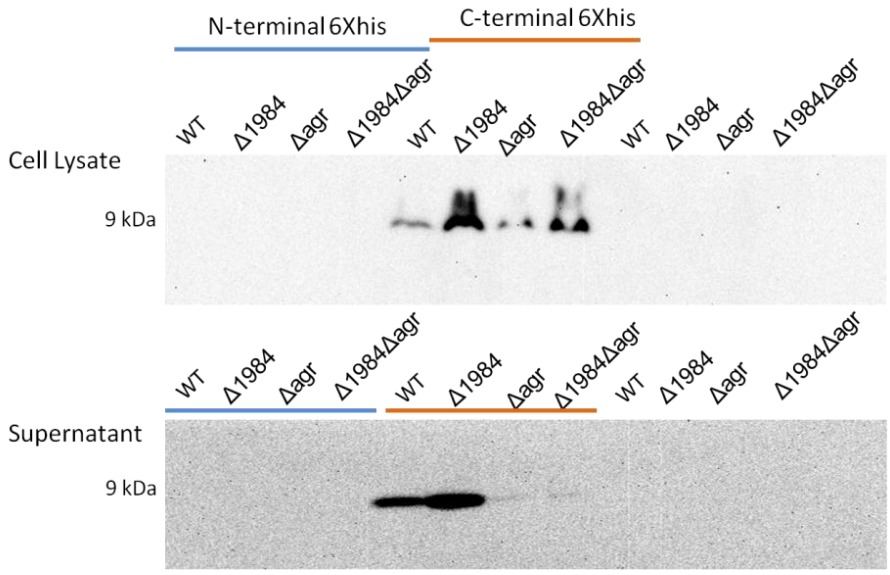

Figure 13. Detection of the C-terminal 6x-histidine-tagged AgrD in whole cell lysates and supernatant. C-terminal 6x-histidine-tagged AgrD is detectable when expression is driven by the pOS1-*pSarA*- sod_{RBS} over- expression plasmid after 8 hours growth in RPMI.

Improving resolution and reproducibility in detection of 6x-His-AgrD by immunoblot. Although I was able to detect C-terminal 6x-His-tagged AgrD, my immunoblot results were not reproducible. I reasoned that the lack of reproducibility could either be due to degradation of the AgrD peptide product or improper immunoblot conditions. Therefore, I continued to repeat these experiments, with the aim of optimizing the resolution of my immunoblots in order to detect possible cleavage events and improve inter-experiment variability. The two major changes I made were to (i) use Tricine-SDS-PAGE gels as described by Schägger to enhance resolution of small peptides less that 10 kDa (59) and (ii) expose my Western blots on film instead of using

the Protein Simple, which routinely gives irregular signal detection when protein abundance is low. Upon incorporation of these experimental changes, my results were much more consistent across experiments. One notable feature of these improved immunoblots was the detection of AgrD in greater abundance in strains lacking *1984* (Figure 14). However, it was still difficult to draw conclusions about alterations in size due to presumed gel overloading and resultant poor resolution (Figure 14). Nonetheless, these data indicated that, in the absence of *1984*, AgrD is present in greater abundance within whole cell lysates and may suggest an important role for 1984 in facilitating localization of AgrD in the cell.

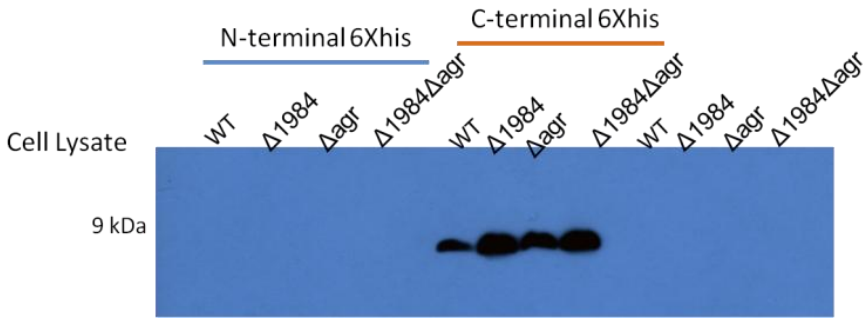

Figure 14. Differences in AgrD cleavage events may be visible when using Tricine-SDS-PAGE gels exposed to film. Representative immunoblot after running protein sample from whole cell lysates on a Tricine-SDS-PAGE gel. Immunoblot exposed to film for 5 minutes.

AgrD processing is altered in Δ*1984*, Δ*agr*, Δ*1984*Δ*agr* mutant backgrounds.

Although I was now able to achieve reproducible immunodetection of C-terminal 6x-His-AgrD, and observed an increased abundance of cell associated AgrD in Δ*1984* mutant backgrounds, I still could not draw firm conclusions on size changes because the immunoblots were overloaded with sample. Based on my results, I hypothesized that my current method of normalizing samples (optical density) was not suitable for detection of shifts in peptide length, due to the increased abundance of AgrD in the lysates of all

strains lacking *1984*. To prevent overloading of the strains, I altered my protocol and began loading gels based on relative abundance of the protein, rather than normalizing to the amount of bacteria present. To further improve resolution, I began running longer gels at a higher percentage of acrylamide in the presence of 6 Molar urea. I anticipated immunoblots conducted with these alterations would improve visualization of shifts in size that might correlate with AgrD processing. This was indeed the case, as the wild type and Δ*1984+1984* samples ran at a discernibly higher molecular weight then the other AgrD species derived from Δ*1984*, Δ*agr* and Δ*1984*Δ*agr* mutants (Figure 15). Although the wild type and Δ*1984+1984* results where unexpected , I suspect the higher molecular weight species in the wild type and Δ*1984+1984* samples could correspond to full length unprocessed AgrD with no detectable processing intermediates. Processing and secretion of AgrD may be happening much faster in these strains and therefore processing intermediates are either secreted or degraded. An alternate possibility is that the visualized band is processed AgrD with an inappropriately formed thiolactone ring, which could potentially affect how the peptide is running through the gel. Nonetheless, these results indicate that a discernable difference in AgrD migration is observed for WT and Δ*1984+1984*, implying *1984* and *agrB* are both influencing peptide processing to some degree.

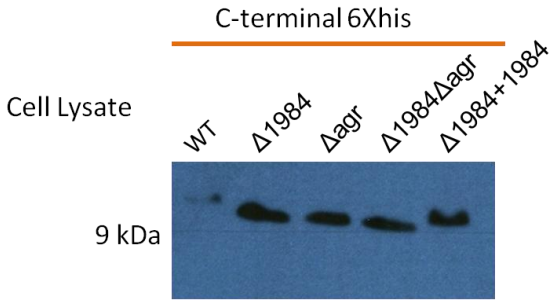

Figure 15. Visualization of AgrD cleavage events is enhanced after normalizing to protein abundance. Representative immunoblot after running protein sample from whole cell lysates on a 21% Tricine-SDS-PAGE gel with 6M urea. Immunoblot exposed to film for 10 minutes.

Improving detection of AgrD processing intermediates. Although I have detected what appear to be alterations in migration associated with C-terminal 6x-His-tagged AgrD derived from different strains, I would have expected to be able to detect processing intermediates present within a single well based on prior studies in the literature. There are several possible explanations for the lack of detection of processing intermediates in my samples. The first possibility is that my sample preparations do not adequately solubilize all AgrD peptide processing intermediates. To overcome the possibility of solubility issues I have attempted alternate whole cell lysate preparations. During these cell lysate preparations I boiled the samples in 6x-SDS buffer before centrifuging out the glass beads and cell debris. By changing the order 6x-SDS addition in this way, I anticipated that I would better solubilize more protein including AgrD intermediates. However, upon generating these preparations, it seems they contained too much cellular debris causing the samples to run unevenly through the gels making determination of shifts in size increasingly difficult (results not shown).

Although I was unable to rule out poor solubility as a cause of undetectable peptide processing intermediates, I hypothesized that the AgrD processing intermediates might alternatively be at too low a concentration, or might be degraded so rapidly that

they are not detected by immunoblot. Therefore, I first attempted to increase the amount of 6x-His-tagged processing intermediates by concentrating my samples using affinity chromatography with nickel resin. However, this method did not yield reproducible detection of 6x-His-tagged AgrD or alternate processing events by immunoblot (results not shown). I then attempted to overcome potential degradative processes by adding protease inhibitor to my lysate preparations. However, the protease inhibitor treatment did not allow for detection of any additional bands by immunoblot (results not shown). Together these data have not been able to conclusively determine the reason for my inability to detect AgrD peptide processing intermediates. While not yet able to draw firm conclusions about peptide processing from these studies, I have set the groundwork for how this experiment will need to be done to yield positive results in the future.

Attempt to detect N-terminal 6x-His-tagged AgrD by immunoblot. Although I was able to successfully detect C-terminal 6x-His-tagged AgrD and potentially ascertain some role for 1984 and AgrB in peptide processing, I have not yet been able to detect N-terminal 6x-His-tagged AgrD under any of the previously described conditions. N-terminal 6x-His-AgrD has been used for immunodetection studies in the literature and was found to be superior to C-terminal 6x-His-tagged AgrD whose processing byproducts are often rapidly degraded. Because N-terminal 6x-His-tagged AgrD was used routinely in studies exploring the AgrB-dependent peptide processing, I returned to the literature to try to understand why I was unable to detect the N-terminal 6x-His-tagged AgrD constructs that I originally generated. Several papers have successfully tagged the N-terminus of AgrD in order to detect peptide processing, but I found that they often required a “linker” between the 6x-His-tag and the N-terminal end of AgrD (11, 12,

58). Based upon this observation, I generated new expression plasmids, still using pOS1-P_{sarA}- sod_{RBS}, but now with a linker region between the 6x-His-tag and AgrD (Figure 12E). I chose to include a 45 nucleotide "S-tag" linker between the 6x-His and AgrD, as this construct had been previously used by Alex Argianas to successfully purify AgrD. I expected that the addition of the linker region would allow for detection of N-terminal 6x-His tagged AgrD by immunoblot. Although incomplete, these results were promising as I was able to detect N-terminal 6x-His-tagged AgrD in a few of the strains tested (Figure 16). Detection of the N-terminal 6x-His-tagged AgrD will need to be further optimized in order to be able to make any conclusions on peptide processing by immunoblot.

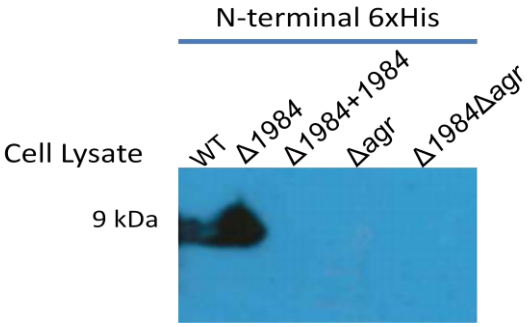

Figure 16. N-terminal 6x-histidine-tag is detectable when there is a linker. Immunoblot after running protein sample from whole cell lysates on a 21% Tricine-SDS-PAGE gel with 6M urea. Immunoblot exposed to film for 5 minutes.

Use of purified AgrD to evaluate 1984-dependent peptide processing. The immunoblots generated using 6x-His-tagged AgrD peptide expression strains do not currently provide sufficient evidence for the involvement of 1984 in AgrD peptide processing. Because we have had difficulties generating sufficient peptide concentration for reliable immunodetection, I decided to attempt an alternate method to determine the involvement of 1984 in AgrD peptide processing. I initiated experiments using membrane fractions from wild type, Δ*1984*, Δ*1984+1984*, Δ*agr*, or Δ*1984*Δ*agr* strains along with

purified AgrD to evaluate cleavage events of the purified peptide. Alex Argianas has been working on purifying AgrD, 1984, and AgrB for use in biochemical studies. I was able to attempt an experiment where I applied partially purified AgrD to membrane fractions in an in vitro cleavage assay. From this assay, I would expect to be able to visualize alterations in AgrD peptide cleavage in a similar manner as the immunoblots described above (see figure 11). Unfortunately, purified AgrD levels were too low in this initial purified preparation to visualize peptide processing by immunoblot (Data not shown). Once we have more concentrated preparations of AgrD to work with these studies can be further optimized.

Assess the role of 1984 in altering immune function during *S. aureus* infection.

Introduction. I have shown increased macrophage secretion of IL-1β *in vitro* after treatment with supernatant derived from a *1984* mutant (Figure 7) and that 1984 is likely involved in AgrD peptide processing (Figure 10). If these phenotypes are recapitulated *in vivo* they could have significant effects on immune cell recruitment and, in turn, bacterial virulence characteristics. For example, IL-1β is a cytokine produced by activated macrophages and is involved in neutrophil recruitment as well as promoting a proinflammatory immune response. Thus, dramatic shifts in IL-1β expression during infection would be expected to dramatically alter the cellular immune environment. Furthermore, if the Agr system is not functioning appropriately, the regulation of virulence factors will no longer maintain optimal expression kinetics. Without this regulation, *S. aureus* can lose its ability to evade immune surveillance mechanisms, thereby compromising its survival *in vivo*. For these reasons, I hypothesize that the

Δ*1984* mutant will be attenuated in multiple *in vivo* infection models similar to a Δ*agr* mutant.

1984 and the Agr system are critical during skin and soft tissue infections. *S. aureus* frequently causes localized disease in the skin and Agr activity is known to be critical for *S. aureus* virulence in the skin of mice (28). Therefore, I used a murine skin and soft tissue infection model to study the involvement of 1984 during *in vivo* infection. This mouse model measures localized infection events that do not easily disseminate. Female ND4 Swiss Webster mice were infected with WT, Δ*1984,* Δ*1984+1984,* and Δ*agr* in the right and left flank, followed by monitoring disease at 72 and 120 hours post-infection. At 72 hours post infection (Figure 17A and C), there was not a significant difference in bacterial CFU recovered from abscess sites between any of the strains tested indicating that Agr and 1984 are likely not involved early in *S. aureus* infection of the skin. Additionally, many of the abscesses at this time point were similar regardless of bacterial strain, although Δ*1984* and Δ*agr* showed a trend toward reduced abscess size (Figure 17C). At 72 hours a larger number of wild type and Δ*1984*+1984 infected abscesses were starting to rupture compared to those infected with a Δ*1984* or Δ*agr* mutant. When we carried the infection out to 120 hours (Figure 17B, D), we saw that a Δ*agr* mutant was significantly attenuated (Figure 17B). Similarly, we saw that a Δ*1984* mutant had significantly decreased CFU in the skin abscesses compared to wild type infected abscesses (Figure 17B). These differences in CFU are clearly reflected by the gross pathology differences observed in the abscesses (Figure 17D). At 120 hours post infection, wild type and Δ*1984+1984*-infected animals had inflamed, dermonecrotic abscesses that had ruptured. In contrast, mice infected with either a Δ*1984* or a Δ*agr*

mutant had very little apparent inflammation in what seem to be resolving abscesses. Serum and skin samples were collected at each time point to analyze cytokine levels by CBA. At 72 hours post infection in the skin, IL-1β levels were higher during infection with a Δ*1984* mutant compared to the others, similar to what we had shown *in vitro* (Figure 18). Although, these results were not statistically significant this trend toward increased IL-1β closely resembles the macrophage cytokine secretion levels seen *in vitro* upon treatment with Δ*1984* supernatant, and may provide some insight into the alterations in immune responses that influence infection kinetics of Δ*1984* infected animals, such as clearance of the bacteria and decreased tissue damage. By 120 hours post-infection both a Δ*1984* and a Δ*agr* mutant had much less IL-1β in their abscesses than wild type and Δ*1984+1984.* Perhaps this modulation of IL-1β secretion early in infection provides evidence for why a Δ*1984* mutant is so readily cleared at 120 hours, as early transient high levels of IL-1β would increase the immune cell recruitment to promote restriction of bacterial infection. At 72 hours, Δ*agr* infected mice did not exhibit increased IL1-β levels, suggesting these two mutants may exhibit differing mechanisms of cytokine induction. On a whole, these data indicate 1984 and Agr are crucial to pathogenesis in a skin and soft tissue infection model. Furthermore, although preliminary, the data are suggestive of a role for IL-1β in the early immune recognition and clearance of *1984* mutant. Additional studies are needed to lend credence to this notion.

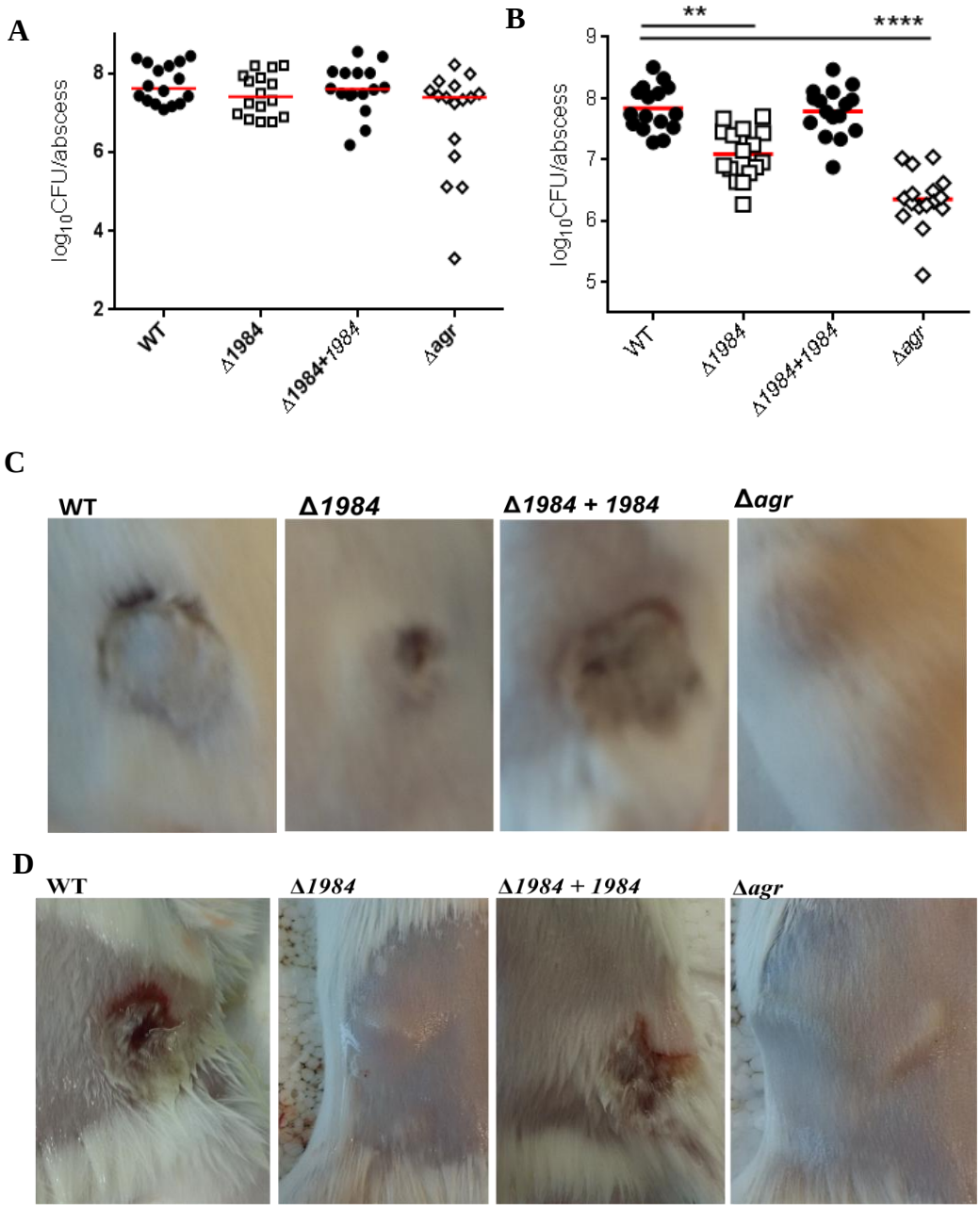

Figure 17. 1984 and the Agr system are critical during skin and soft tissue infections. A skin and soft tissue infection model was used in which mice were infected intradermally with $1x10^7$ CFU of bacteria in the presence of Cytodex beads in both the right and left flank. 72 hours (A) or 120 hours (B) post-infection mice were sacrificed and skin abscesses were collected to enumerate CFU. Representative abscesses (C) and (D) 120 hours post infection. Each experiment contained cohorts of 4 mice and was performed twice. Statistical analysis was a Kruskal-wallis test. ** P= 0.0052 and **** P<0.0001.

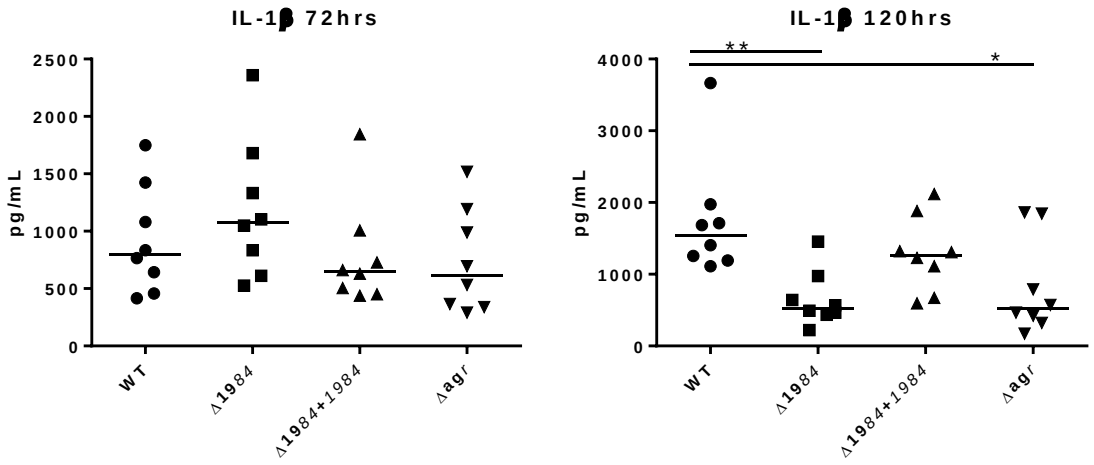

Figure 18. A Δ*1984* mutant leads to a heightened amount of IL-1β in skin abscesses early in infection. Abscess homogenates were collected and CBA was performed. One representative experiment is shown. Each experiment contained cohorts of 4 mice with two abscesses per mouse and was performed twice. A one-way Anova was used to test for significance of the data.

A Δ*1984* mutant does not behave like a Δ*agr* mutant during a peritonitis model of infection. Using a skin and soft tissue model of infection allowed us to determine that a Δ*1984* mutant as well as a a Δ*agr* mutant are significantly attenuated in a localized infection model. However this model does not sufficiently test the effects these mutations have on dissemination. *S. aureus*-induced peritonitis is an alternative infection model that can measure infection kinetics as well as dissemination to distal target organs and immune cell recruitment in a way the skin and soft tissue infection models cannot. Therefore, use of this model in my studies should provide additional information on the role of 1984 during more complex infectious scenarios where dissemination is important to pathobiology. A Δ*agr* mutant is significantly attenuated in the mouse peritonitis model, therefore if a Δ*1984* mutant were attenuated in vivo due to its deleterious effects on Agr signaling, I would expect a Δ*1984* mutant to be attenuated to a similar degree. To my surprise, a Δ*1984* mutant did not phenocopy a Δ*agr* mutant. Although a Δ*1984* mutant is slightly attenuated in the peritoneal cavity, it is not attenuated to the same

degree as Δ*agr* mutant (Figure 19). Furthermore, a Δ*1984* mutant shows signs of hypervirulence in the kidneys as evidenced by a modest, but not statistically significant, increase in CFU compared to the wild type strain (Figure 19). Serum and peritoneal lavage fluid were collected to measure cytokine levels and immune cells were isolated from lavage fluid and lymph nodes for flow cytometry analysis of immune cell recruitment to each site. The results from cytokine measurements and immune cell recruitment were inconclusive as these experiments produced a wide variability in results (data not shown). Together, these results demonstrated that, in the absence of 1984, *S. aureus* is not markedly attenuated during peritonitis. In contrast, a *agr* mutant is significantly attenuated. This discrepancy in pathogenic outcomes between a Δ*1984* and Δ*agr* mutant may be indicative of roles for 1984 in vivo that extend beyond its contribution to Agr system activation.

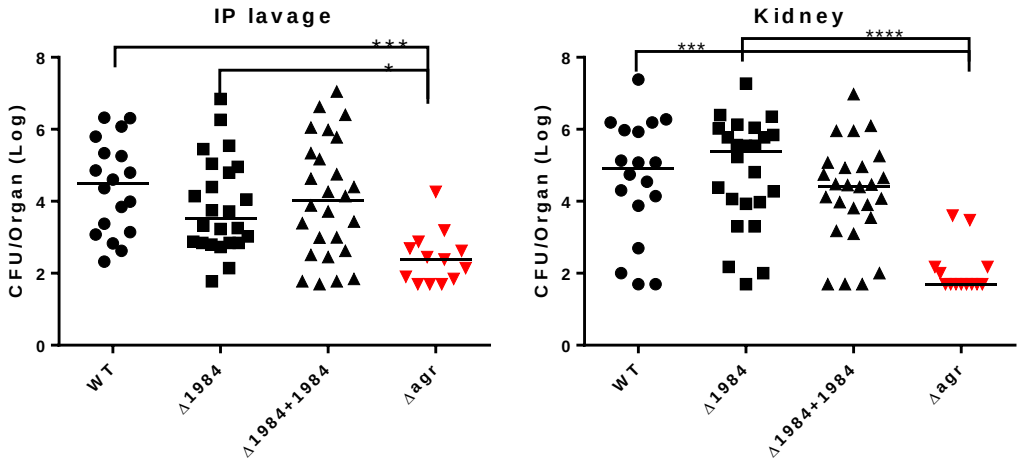

Figure 19. A Δ*1984* mutant does not behave like a Δ*agr* mutant during a peritonitis model of infection. Mice were infected IP with $1x10^8$ CFU of bacteria and euthanized 72 hours post infection. Each experiment contained cohorts of at least 4 mice and was repeated at least 3 times. A kruxkal-Wallis test was perfomed to determine significance of the data.

A Δ*1984* mutant does not behave like a Δ*agr* mutant during a systemic model of infection. Since we have extensively evaluated the contribution of 1984 activity in localized infection models, it was important to also examine the effect a Δ*1984* mutant during systemic infection (sepsis). A systemic infection model is clinically relevant as it mimics the direct seeding of the bloodstream that can happen after invasive surgery or during intravenous drug use. Using this model, we can evaluate tissue seeding and replication without the bottleneck to dissemination that occurs during localized infection of the skin and peritonitis. In this model, a Δ*agr* mutant typically exhibits modest attenuation in the kidney. My data recapitulate these results, as a Δ*agr* mutant exhibited approximately 0.5 log reduction in CFU in the kidney compared to wild type *S. aureus* (Figure 20) 96 hours post-infection. In contrast, a Δ*1984* mutant was not attenuated in the kidney (Figure 20). In fact, the Δ*1984* mutant had a marked, but not statistically significant, increase in CFU in the heart compared to wild type *S. aureus*. These results indicate that some characteristics of a Δ*1984* mutant *in vivo* are clearly distinct from that of a Δ*agr* mutant.

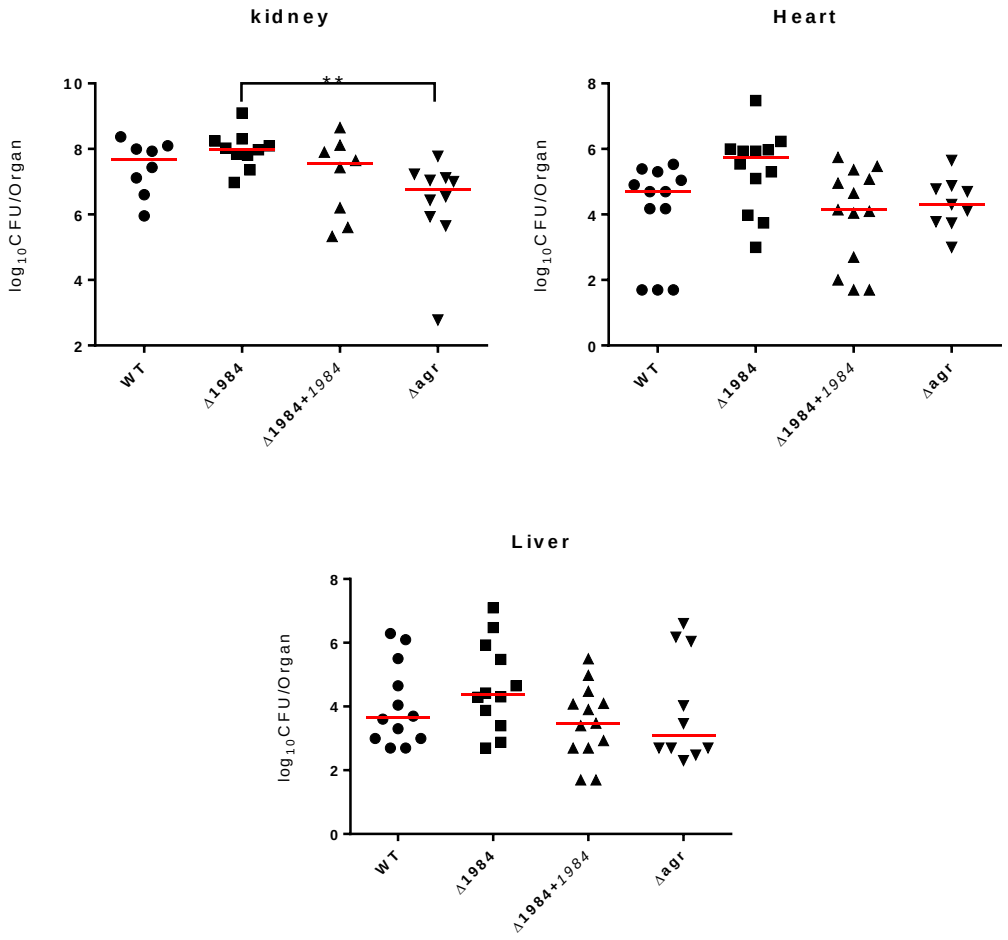

Figure 20. A Δ*1984* mutant does not behave like a Δ*agr* mutant during a systemic model of infection. A systemic model of infection was used in which mice were infected with $1x10^7$ CFU of bacteria by retro-orbital injection and 96 hours post-infection mice were sacrificed and organs were collected. Each experiment contained cohorts of at least 4 mice and was repeated 3 times. A Kruskal-Wallis test was performed to determine significance. Heart and Liver comparisons were not significant.

Δ*1984* derived supernatants contain a unique protein compared to a Δ*agr* mutant. Taken together, the different virulence phenotypes I witnessed between a Δ*1984* mutant and a Δ*agr* mutant during systemic infection and peritonitis were surprising since, in all other conditions, a Δ*1984* mutant closely resembled a Δ*agr* mutant. My results suggest two possible hypotheses. First, in a Δ*1984* mutant there may exist AgrD-independent activation mechanisms *in vivo* that lead to the production of the virulence

factors typically under Agr control. Such an outcome would explain the lack of virulence defect during peritonitis and systemic infection. A second hypothesis is that there is an additional function associated with 1984 that is not related to Agr, which prevents attenuation in vivo when 1984 is absent. One piece of evidence in support of this second hypothesis comes from the exoprotein profiles of a Δ*1984* mutant compared to that of a Δ*agr* mutant (Figure 6) grown in defined medium (RPMI). There is one protein band present in a Δ*1984* mutant that is not present in a Δ*agr* mutant that runs at around 27 kDa in an SDS-PAGE gel. To begin to understand this difference between a Δ*1984* mutant and a Δ*agr* mutant I first completed an eight hour growth curve in which I collected samples every two hours in order to look at the exoprotein profiles of wild type, Δ*1984,* Δ*1984+1984*, and Δ*agr* strains. The presumptive band is apparent in the first four hours of growth of all strains. However, by hour 6 the band was no longer present in the exoprotein profile of any strain except for the samples from a Δ*1984* mutant (Figure 21). Therefore, I identified this protein by mass spectrometry and the results came back with one statistically significant match, the immunodominant *Staphylococcus* antigen A or IsaA (60, 61). IsaA was only present in the supernatant of a Δ*1984* mutant and was not identified in the wild type sample. IsaA is a soluble lytic transglycosylase that was first discovered as an antigen that leads to the production of an immense amount of antibody in infected patients (60). A hyperinflammatory immune response is triggered by the recognition of peptidoglycan released by IsaA during cell division (62). It is also worth noting that IsaA is not regulated by the Agr system (62). A Δ*1984* mutant mimics the deficiencies we see in secretion caused by a Δ*agr* mutant except for IsaA production. Thus, it does not seem IsaA upregulation is related to the roles of 1984 in Agr system

activation. These data provide insights into unique alterations in secreted proteins of a Δ*1984* mutant that have direct links to virulence and that are not seen for a Δ*agr* mutant.

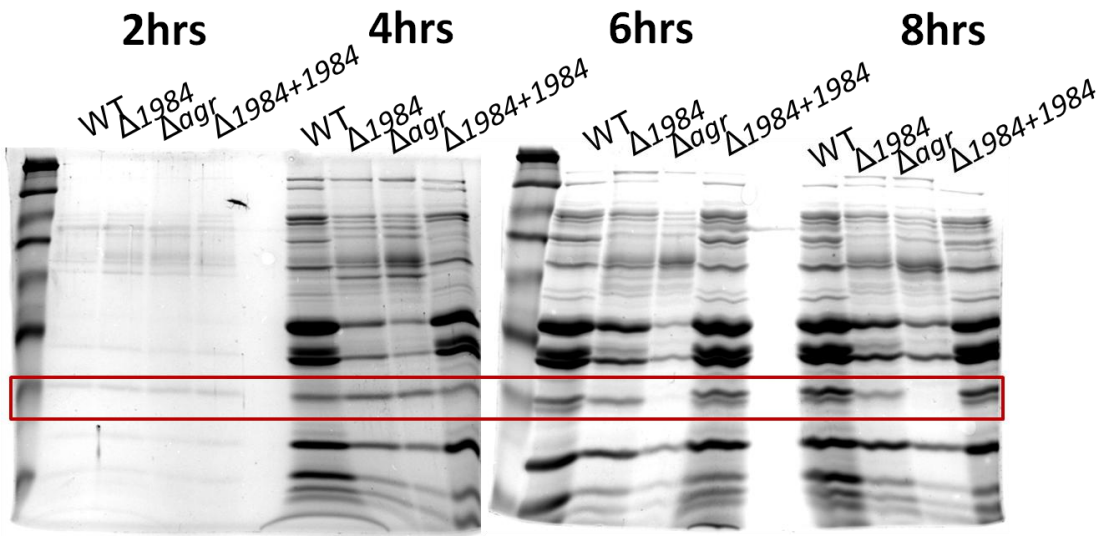

Figure 21. Identification of protein present in supernatant of a Δ*1984* mutant and not in a Δ*agr* mutant. Samples were grown in RPMI, at 37°C with shaking at 200 rpm. Suppernatants were collected every 2 hours for 8 hours. The red box highlights the area of the protein of interest.

Conclusions

I have shown that a Δ*1984* mutant displays phenotypes similar to a Δ*agr* mutant including defects in protein secretion, reduction of virulence factor expression, and altered macrophage activation. On a whole I submit that my findings help support the hypothesis that 1984 is involved in cleaving the N-terminal end of the AgrD peptide in order for *S. aureus* to produce functional AIP. Additionally, The virulence characteristics I have observed for a Δ*1984* mutant in multiple *in vivo* studies have provided a unique perspective into our understanding of the complex functions of 1984 during infection as well as provide future avenues for the lab to explore.

CHAPTER FOUR

DISCUSSION

1984 is a putative peptidase involved in the processing of key signaling peptides.

The goal of this thesis was to investigate the role of 1984 in *S. aureus* quorum sensing and pathogenesis. My studies have revealed that 1984 plays a major role in facilitating quorum sensing, potentially peptide processing, and modulation of the immune response. Using an in-frame deletion mutant of *1984*, I have demonstrated phenotypic similarities to a mutant in a major quorum sensing system in *S. aureus* involved in regulation of surface proteins and secreted virulence factor gene expression. A Δ*1984* mutant phenocopies a Δ*agr* mutant for defects in protein secretion, virulence factor production, and modulation of macrophage cytokine secretion. At this point the assessment of these phenotypic similarities are purely qualitative, therefore quantification by measuring relative virulence factor abundance in western blots as well as quantification of hemolytic activity using numerical methods is warranted. Additionally, 1984 is predicted to have peptidase function. Based on this information, I hypothesized that 1984 is involved in processing AgrD by cleaving the N-terminal end of the peptide. Although I have not obtained direct evidence that 1984 is involved in cleaving the N-terminus of AgrD during AIP processing, I have shown that a Δ*1984* mutant is unable to produce functional AIP.

Visualizing AgrD cleavage by immunoblot.

Over the course of this study, I attempted to visualize AgrD cleavage events using strains containing 6x-histidine-tagged AgrD expression plasmids (Figure 11). Unfortunately, this proved to be more difficult and complex than anticipated. First, I had trouble detecting the 6x-histidine-tagged AgrD until I used a multi-copy plasmid containing a highly expressed promoter and an optimized ribosomal binding site. Using this C-terminal 6x-histidine-tagged AgrD overexpression plasmid, I was able to reproducibly detect AgrD-6x-His by immunoblot. However, peptide cleavage activity was difficult to interpret. Rather than detecting the smallest peptide in the wild type and Δ*1984+1984* samples, which would correspond to C-terminal/fully processed peptide, we detected a band running at a higher molecular weight compared to Δ*1984*, Δ*agr*, or Δ*1984*Δ*agr*. We hypothesize this band corresponds to either full length unprocessed AgrD with no detectable processing intermediates, or processed AIP containing inappropriately formed thiolactone ring (Figure 14). Upon further examination of the literature, the lack of a small molecular weight C-terminal peptide fragment may fit with the necessity for rapid degradation of the C-terminal cleavage product before additional AIP can be produced (18). Additionally, I have attempted to process my samples in the presence of a protease inhibitor. However, this did not allow for detection of additional cleavage products. I hypothesize that this method was ineffective as the degradation could have already occurred during the eight hours of growth, leaving too low a concentration of processing intermediates to be detected by immunoblot. An alternative approach would be to add protease inhibitor during the eight hour incubation. However, this may lead to inhibition of AgrD processing or even inhibit growth. Therefore, this

approach may not be feasible. However, it is also possible that inappropriate thiolactone ring formation could cause the peptide to aberrantly run in the gel, as this modification may not be denatured under the current conditions.

I have found that a linker region between the 6x-histidine-tag and the N-terminal end of AgrD is needed in order to detect the N-terminal tagged AgrD. I predict an N-terminally tagged AgrD may bypass the issues with visualizing C-terminally tagged AgrD and should provide us with direct evidence as to whether or not 1984 is involved in cleaving the N-terminal end of AgrD. N-terminal 6x-histidine-tagged AgrD has been used frequently in similar experiments and the literature suggests the N-terminal end of AgrD does not seem to degrade as quickly compared to the C-terminus (22).

Additionally, Alex Argianas has been working on purifying AgrD, 1984, and AgrB for use in biochemical studies that would also provide evidence for the function of 1984 during AgrD processing. Although it remains to be determined, my recently optimized immunoblot techniques for visualizing 6x-histidine-tagged AgrD; the construction of a potentially detectable N-terminally tagged AgrD peptide; as well as the work being done by Alex Argianas will allow us to directly ascertain whether or not 1984 acts to process the N-terminal portion of the AgrD peptide to produce functional AIP.

1984 homologs exist in other Agr-containing bacteria.

As Agr systems are used by many different bacterial species, I wanted to investigate if 1984 homologs existed in these species. I searched NCBI for homologs to 1984 at the amino acid level in other bacterial species that also have Agr systems and found that other pathogenic and non-pathogenic species also contain 1984 homologs. Additional *Staphylococcal* species that contain highly similar 1984 homologs include

Staphylococcus haemolyticus (90%), *Staphylococcus epidermidis* (65%), and *Staphylococcus saprophyticus* (51%) (Table3). Other pathogenic bacterial species that contain Agr systems also have 1984 homologs, such as *Listeria monocytogenes* (37%), *Enterococus faecalis* (54%), *Clostridium perfringens* (39%), and *Bacillus cereus* (35%). Additionally, non-pathogenic Agr-containing species such as *Listeria innocua* (43%), *Bacillus halodurans* (36%), *Lactobacillus plantarum* (36%), and *Clostridium beijerinckii* (30%) also seem to have homologs for 1984. Although the Agr system in *S. aureus* has been well studied, the potential involvement of 1984 as a conserved peptidase that contributes to the activity of other Agr systems in other bacteria that are less well characterized is an intriguing possibility (63). It would be interesting and important to identify whether or not these homologs behave like 1984 and if they are involved in AgrD processing in these other species.

Bacteria	**Percent Identity**
Staphylococcus haemolyticus	90%
Staphylococcus epidermidis	65%
Staphylococcus saprophyticus	51%
Listeria monocytogenes	37%
Enterococus faecalis	54%
Clostridium perfringens	39%
Bacillus cereas	35%
Listeria innocus	43%
Bacillus halodurans	36%
Lactobacillus plantarum	36%
Clostridium beijerinckii	30%

Table 3. 1984 homologs in other bacterial species.

A Δ*1984* mutant is attenuated during a skin and soft tissue model of infection.

Early during skin and soft tissue infection there is an increase in IL-1β in abscesses infected with a Δ*1984* mutant compared to wild type *S. aureus*. The increase in this pro-inflammatory cytokine could lead to enhanced immune cell recruitment, including neutrophils and other innate cells. With the increase in professional phagocytes more Δ*1984* would be phagocytosed, and without the production of virulence factors regulated by the Agr system this mutant would not be able to escape the phagosome or lyse the cells (41, 42). Therefore I suspect the kinetics of IL-1β release in relation to bacterial clearance from an abscess may be a clear indicator of the mechanism by which a Δ*1984* mutant is attenuated in vivo. However, this requires further exploration. I envision a deeper investigation and quantification of immune cell recruitment and inflammation over a time course using histopathology and immunohistochemistry would help us to better explore the immune activation elicited by a Δ*1984* mutant. By looking over a wider time course, with more time points than the two assessed during this study we may be able to provide insights into the reasons for such a dramatic attenuation of a Δ*1984* mutant and a Δ*agr* mutant during skin and soft tissue infection as well as gain insight into the different infection kinetics of these two mutants.

A Δ*1984* mutant is not attenuated in other infection models.

Despite the similarities we have shown between a Δ*1984* mutant and a Δ*agr* mutant for defects in protein secretion and virulence factor regulation *in vitro*, I have shown that a Δ*1984* mutant is not attenuated like a Δ*agr* mutant during systemic infection and peritonitis. This may indicate that 1984 would not be a good drug target for these infectious scenarios as a Δ*1984* mutant is actually hyper-virulent in certain sites during

peritonitis and systemic infection. Furthermore, these results suggest two possible hypotheses; (i) in a Δ*1984* mutant there may be an AgrD-independent activation mechanism *in vivo* that leads to the production of the virulence factors typically under Agr control and (ii) there is an additional function associated with 1984 that is not related to Agr system activity. Although I haven't ruled out the first possibility, I do have evidence to support the second hypothesis. When examining the secreted protein profiles from wild type, Δ*1984,* and Δ*agr,* I identified an additional protein band present in supernatant from a Δ*1984* mutant and not in the supernatant from a Δ*agr* mutant. This protein has been tentatively identified as the Immunodominant *Staphylococcus* antigen A, IsaA (60, 61). IsaA is a soluble lytic transglycosylase involved in cell division. Furthermore, IsaA is believed to trigger a hyperinflammatory response because during cell division IsaA is predicted to release peptidocglycan, which can be recognized by the components of the immune system. My data suggest that IsaA is down regulated in wild type *S. aureus* within 6 hours of growth but is highly expressed in a Δ*1984* mutant (Figure 21). Additionally, IsaA expression is not under Agr control but is positively regulated by SarA and YycFG, which are two additional regulators in *S. aureus* (62). IsaA regulation is complex, but it does not seem that IsaA up regulation in a Δ*1984* mutant is related to the role of 1984 in Agr system activation as we do not see an upregulation of IsaA in a Δ*agr* mutant and *isaA* is not known to be regulated by Agr.

Although preliminary, the identification of significant amounts of IsaA in Δ*1984* supernatant may allude to a role for this product in the altered infection kinetics we have seen for a Δ*1984* mutant during peritonitis and systemic models of infection. To confirm that the band is IsaA I would want to make a clean mutation in a Δ*1984* mutant

background. I could then coomassie stain the exoprotein profile. If the band is IsaA, then the band would be no longer be present in a Δ*1984*Δ*IsaA* mutant. To test the role of IsaA during infection with a Δ*1984* mutant, I would make a Δ*1984*Δ*isaA* double mutant and repeat the systemic and peritonitis infection models. If the upregulation of IsaA is responsible for the difference in virulence we see between a Δ*1984* mutant and a Δ*agr* mutant during peritoneal and systemic infection models, then I would expect this additional mutation would restore a Δ*1984* mutant to similar levels of attenuation as a Δ*agr* mutant in these infection models. The interactions between 1984 and IsaA provide another unique and interesting relationship to examine in future work.

Clinical therapeutic implication of quorum quenching therapies to treat *S. aureus.*

Increased incidence of antibiotic resistance among infectious isolates of *S. aureus* has necessitated discussion of new drug targets and new therapies. A Δ*agr* mutant is significantly attenuated during skin and soft tissue as well as peritonitis models of infection. This would suggest that targeting the Agr quorum sensing system may be an effective drug target. However, the hyper-virulence of a Δ*1984* mutant in peritonitis and systemic infection models suggests 1984, and perhaps Agr, would not be an optimal drug target for treatment of invasive disease. Nevertheless, quorum quenching therapeutics that target Agr have been pursued by a number of research laboratories. The use of quorum quenching therapeutics relies on three key criteria. The first is that the quorum sensing system is actively used during infection for virulence (64). Based on the data presented here, it seems the Agr system is critically involved in pathogenesis during certain infectious conditions, but not others. Thus, the Agr system partially meets this criterion. The second assumption is that the quorum sensing system is not essential for

bacterial growth; therefore there will be less selective pressure for the bacteria to develop resistance against the therapy (7, 64). A Δ*agr* deletion mutant does not have any growth defects, therefore the Agr system meets this criterion as well. The final assumption is that the therapy would be species specific to reduce the off-target effects associated with antibiotics (64). For example, currently, antibiotic treatment can have serious effects on microbiota homeostasis. The Agr system is remarkably specific and AgrD peptides often act only on certain subsets of *S. aureus* strains. Therefore, the AgrD system fulfills this final criterion as well.

Given that the Agr system fulfills all primary criteria needed to support the design of quorum quenching inhibitors it is not surprising that a significant body of research exists toward achieving this goal. One proposed method of Agr system targeting is sequestration of the signal peptide, AIP, using antibodies (64). An issue with this method is that the antibodies used are often highly specific for one Agr group, therefore it would not be effective against all *S. aureus* strains. This caveat aside, co-administration studies with bacteria and AIP-specific antibody does prevent lesion formation in a murine subcutaneous infection model (65). Additionally, passive immunization with AIP antibodies limits pathogenicity during lethal challenge (65). Another approach to quorum quenching is to target the functionality of the system. One chemical inhibitor, savirin, binds to AgrA, preventing its function (66). In experimental studies savirin treatment did not provoke a stress response by the bacteria and therefore is not believed to constitute a significant selective pressure for *S. aureus* to develop resistance. Nonetheless, an effective therapeutic derived from savirin has not been realized. Other researchers have attempted to use proteases as quorum quenching treatments, but proteases tend to have

broad specificity making enzymatic degradation of peptides a non-ideal treatment option, as there may be off-target effects (64). Yet another possible quorum quenching therapy for the Agr system may lie in the fact that there are four Agr groups with specific sequences and specificity (15, 16). These variants can interfere with and inhibit the function of other Agr groups. It is predicted that the different variants may isolate bacterial populations through niche competition (7). Thus peptide analogues of these Agr groups could be used as a quorum quenching therapy. For example, it has been shown that synthetic AIP-II reduces abscess formation when coadministered with an infecting group I *S. aureus* isolate (19). The downside to AIP group-specific inhibition is that these treatments are only efficacious against specific strain subsets that harbor the opposing AIP.

A broad treatment that could act against all Agr groups would be a more favorable mechanism of quorum quenching over that of group specific inhibition. For example, Lyon et al. created trAIP-II derived from group II AIP lacking the exocyclic tail (67). They were able to show that this molecule is able to inhibit all four Agr groups. Although this potential therapeutic seems promising, it is important to note that Agr defective *S. aureus* are detected in colonizing isolates, as well as isolates associated with infection persistence and bacteremia. These findings indicate that naturally occurring Agr mutants with infectious potential do still occur in the human host potentially hampering the therapeutic potential of quorum quenching inhibitors (7). Based on information in the literature, the Agr system is required during acute infection, but during chronic infection there is selection for *agr* mutants because these variants have increased biofilm formation, antibiotic resistance, and long-term persistence capabilities (7). This suggests

that the use of the Agr system as a treatment target may only be effective during certain infectious scenarios (acute disease) or certain infectious sites (skin abscess formation).

Conclusions.

Although this work has not fully defined the roles of 1984 during *S. aureus* pathogenesis or gene regulation, we have begun to elucidate its complex functions and interactions with major quorum sensing circuitry. This work has provided the lab with techniques that will allow further study of the involvement of 1984 in promoting optimal Agr system activity. Furthermore, I have provided the lab future avenues to explore in order to expand on our understanding of the complex functions 1984 may play during infection.

REFRENCE LIST

1. Klein E, Smith DL, Laxminarayan R. Hospitalizations and deaths caused by methicillin-resistant *Staphylococcus aureus*, United States, 1999-2005. Emerg Infect Dis. 2007 Dec;13(12):1840-6.

2. Lowy FD. *Staphylococcus aureus* Infections. N Engl J Med. 1998 08/20; 2015/07;339(8):520-32.

3. Klevens RM, Morrison MA, Nadle J, Petit S, Gershman K, Ray S, et al. Invasive methicillin-resistant *Staphylococcus aureus* infections in the United States. JAMA. 2007 Oct 17;298(15):1763-71.

4. Noble WC, Valkenburg HA, Wolters CH. Carriage of *Staphylococcus aureus* in random samples of a normal population. J Hyg (Lond). 1967 Dec;65(4):567-73.

5. Spaan AN, Surewaard BG, Nijland R, van Strijp JA. Neutrophils versus *Staphylococcus aureus*: a biological tug of war. Annu Rev Microbiol. 2013;67:629-50.

6. Skrupky LP, Micek ST, Kollef MH. Bench-to-bedside review: Understanding the impact of resistance and virulence factors on methicillin-resistant *Staphylococcus aureus* infections in the intensive care unit. Crit Care. 2009;13(5):222.

7. Bronesky D, Wu Z, Marzi S, Walter P, Geissmann T, Moreau K, et al. *Staphylococcus aureus* RNAIII and Its Regulon Link Quorum Sensing, Stress Responses, Metabolic Adaptation, and Regulation of Virulence Gene Expression. Annu Rev Microbiol. 2016 Jul 6.

8. Ji G, Beavis RC, Novick RP. Cell density control of staphylococcal virulence mediated by an octapeptide pheromone. Proc Natl Acad Sci U S A. 1995 Dec 19;92(26):12055-9.

9. Koenig RL, Ray JL, Maleki SJ, Smeltzer MS, Hurlburt BK. *Staphylococcus aureus* AgrA binding to the RNAIII-agr regulatory region. J Bacteriol. 2004 Nov;186(22):7549-55.

10. Zhang L, Ji G. Identification of a staphylococcal AgrB segment(s) responsible for group-specific processing of AgrD by gene swapping. J Bacteriol. 2004 Oct;186(20):6706-13

11. Zhang L, Gray L, Novick RP, Ji G. Transmembrane topology of AgrB, the protein involved in the post-translational modification of AgrD in *Staphylococcus aureus*. J Biol Chem. 2002 Sep 20;277(38):34736-42.

12. Qiu R, Pei W, Zhang L, Lin J, Ji G. Identification of the putative staphylococcal AgrB catalytic residues involving the proteolytic cleavage of AgrD to generate autoinducing peptide. J Biol Chem. 2005 Apr 29;280(17):16695-704.

13. Thoendel M, Horswill AR. Random mutagenesis and topology analysis of the autoinducing peptide biosynthesis proteins in *Staphylococcus aureus*. Mol Microbiol. 2013 Jan;87(2):318-37.

14. Lina G, Jarraud S, Ji G, Greenland T, Pedraza A, Etienne J, et al. Transmembrane topology and histidine protein kinase activity of AgrC, the agr signal receptor in *Staphylococcus aureus*. Mol Microbiol. 1998 May;28(3):655-62.

15. Jarraud S, Lyon GJ, Figueiredo AM, Lina G, Vandenesch F, Etienne J, et al. Exfoliatin-producing strains define a fourth agr specificity group in *Staphylococcus aureus*. J Bacteriol. 2000 Nov;182(22):6517-22.

16. Ji G, Beavis R, Novick RP. Bacterial interference caused by autoinducing peptide variants. Science. 1997 Jun 27;276(5321):2027-30.

17. Zhang L, Lin J, Ji G. Membrane anchoring of the AgrD N-terminal amphipathic region is required for its processing to produce a quorum-sensing pheromone in *Staphylococcus aureus*. J Biol Chem. 2004 May 7;279(19):19448-56.

18. Wang B, Zhao A, Novick RP, Muir TW. Key driving forces in the biosynthesis of autoinducing peptides required for staphylococcal virulence. Proc Natl Acad Sci U S A. 2015 Aug 25;112(34):10679-84.

19. Mayville P, Ji G, Beavis R, Yang H, Goger M, Novick RP, et al. Structure-activity analysis of synthetic autoinducing thiolactone peptides from *Staphylococcus aureus* responsible for virulence. Proc Natl Acad Sci U S A. 1999 Feb 16;96(4):1218-23.

20. Novick RP, Geisinger E. Quorum sensing in staphylococci. Annu Rev Genet. 2008;42:541-64.

21. Wang B, Muir TW. Regulation of Virulence in *Staphylococcus aureus*: Molecular Mechanisms and Remaining Puzzles. Cell Chem Biol. 2016 Feb 18;23(2):214-24.

22. Gonzalez DJ, Corriden R, Akong-Moore K, Olson J, Dorrestein PC, Nizet V. N-terminal ArgD peptides from the classical *Staphylococcus aureus* Agr system have cytotoxic and proinflammatory activities. Chem Biol. 2014 Nov 20;21(11):1457-62.

23. Kavanaugh JS, Thoendel M, Horswill AR. A role for type I signal peptidase in *Staphylococcus aureus* quorum sensing. Mol Microbiol. 2007 Aug;65(3):780-98.

24. Nikolskaya AN, Galperin MY. A novel type of conserved DNA-binding domain in the transcriptional regulators of the AlgR/AgrA/LytR family. Nucleic Acids Res. 2002 Jun 1;30(11):2453-9.

25. Novick RP, Ross HF, Projan SJ, Kornblum J, Kreiswirth B, Moghazeh S. Synthesis of staphylococcal virulence factors is controlled by a regulatory RNA molecule. EMBO J. 1993 Oct;12(10):3967-75.

26. Boisset S, Geissmann T, Huntzinger E, Fechter P, Bendridi N, Possedko M, et al. *Staphylococcus aureus* RNAIII coordinately represses the synthesis of virulence factors and the transcription regulator Rot by an antisense mechanism. Genes Dev. 2007 Jun 1;21(11):1353-66.

27. Falugi F, Kim HK, Missiakas DM, Schneewind O. Role of protein A in the evasion of host adaptive immune responses by *Staphylococcus aureus*. MBio. 2013 Aug 27;4(5):e00575-13.

28. Lacey KA, Geoghegan JA, McLoughlin RM. The Role of *Staphylococcus aureus* Virulence Factors in Skin Infection and Their Potential as Vaccine Antigens. Pathogens. 2016 Feb 17;5(1):10.3390/pathogens5010022.

29. Sjodahl J. Repetitive sequences in protein A from *Staphylococcus aureus*. Arrangement of five regions within the protein, four being highly homologous and Fc-binding. Eur J Biochem. 1977 Mar 1;73(2):343-51.

30. Goodyear CS, Silverman GJ. Death by a B cell superantigen: In vivo VH-targeted apoptotic supraclonal B cell deletion by a Staphylococcal Toxin. J Exp Med. 2003 May 5;197(9):1125-39.

31. Powers ME, Becker RE, Sailer A, Turner JR, Bubeck Wardenburg J. Synergistic Action of *Staphylococcus aureus* alpha-Toxin on Platelets and Myeloid Lineage Cells Contributes to Lethal Sepsis. Cell Host Microbe. 2015 Jun 10;17(6):775-87.

32. Wilke GA, Bubeck Wardenburg J. Role of a disintegrin and metalloprotease 10 in *Staphylococcus aureus* alpha-hemolysin-mediated cellular injury. Proc Natl Acad Sci U S A. 2010 Jul 27;107(30):13473-8.

33. Becker RE, Berube BJ, Sampedro GR, DeDent AC, Bubeck Wardenburg J. Tissue-specific patterning of host innate immune responses by *Staphylococcus aureus* alpha-toxin. J Innate Immun. 2014;6(5):619-31.

34. Thammavongsa V, Kim HK, Missiakas D, Schneewind O. Staphylococcal manipulation of host immune responses. Nat Rev Microbiol. 2015 Sep;13(9):529-43.

35. Alonzo F,3rd, Torres VJ. Bacterial survival amidst an immune onslaught: the contribution of the *Staphylococcus aureus* leukotoxins. PLoS Pathog. 2013 Feb;9(2):e1003143.

36. Reyes-Robles T, Alonzo F,3rd, Kozhaya L, Lacy DB, Unutmaz D, Torres VJ. *Staphylococcus aureus* leukotoxin ED targets the chemokine receptors CXCR1 and CXCR2 to kill leukocytes and promote infection. Cell Host Microbe. 2013 Oct 16;14(4):453-9.

37. Cheung GY, Duong AC, Otto M. Direct and synergistic hemolysis caused by *Staphylococcus* phenol-soluble modulins: implications for diagnosis and pathogenesis. Microbes Infect. 2012 Apr;14(4):380-6.

38. Schwartz K, Syed AK, Stephenson RE, Rickard AH, Boles BR. Functional amyloids composed of phenol soluble modulins stabilize *Staphylococcus aureus* biofilms. PLoS Pathog. 2012;8(6):e1002744.

39. Rautenberg M, Joo HS, Otto M, Peschel A. Neutrophil responses to staphylococcal pathogens and commensals via the formyl peptide receptor 2 relates to phenol-soluble modulin release and virulence. FASEB J. 2011 Apr;25(4):1254-63.

40. Queck SY, Jameson-Lee M, Villaruz AE, Bach TH, Khan BA, Sturdevant DE, et al. RNAIII-independent target gene control by the agr quorum-sensing system: insight into the evolution of virulence regulation in *Staphylococcus aureus*. Mol Cell. 2008 Oct 10;32(1):150-8.

41. Munzenmayer L, Geiger T, Daiber E, Schulte B, Autenrieth SE, Fraunholz M, et al. Influence of Sae and Agr regulated factors on the escape of *Staphylococcus aureus* from human macrophages. Cell Microbiol. 2016 Feb 19.

42. O'Keeffe KM, Wilk MM, Leech JM, Murphy AG, Laabei M, Monk IR, et al. Manipulation of Autophagy in Phagocytes Facilitates *Staphylococcus aureus* Bloodstream Infection. Infect Immun. 2015 Sep;83(9):3445-57.

43. Chopin MC, Chopin A, Bidnenko E. Phage abortive infection in lactococci: variations on a theme. Curr Opin Microbiol. 2005 Aug;8(4):473-9.

44. Haaber J, Samson JE, Labrie SJ, Campanacci V, Cambillau C, Moineau S, et al. Lactococcal abortive infection protein AbiV interacts directly with the phage protein SaV and prevents translation of phage proteins. Appl Environ Microbiol. 2010 Nov;76(21):7085-92.

45. Frankel MB, Wojcik BM, DeDent AC, Missiakas DM, Schneewind O. ABI domain-containing proteins contribute to surface protein display and cell division in *Staphylococcus aureus*. Mol Microbiol. 2010 Oct;78(1):238-52.

46. Kjos M, Snipen L, Salehian Z, Nes IF, Diep DB. The abi proteins and their involvement in bacteriocin self-immunity. J Bacteriol. 2010 Apr;192(8):2068-76.

47. Parma DH, Snyder M, Sobolevski S, Nawroz M, Brody E, Gold L. The Rex system of bacteriophage lambda: tolerance and altruistic cell death. Genes Dev. 1992 Mar;6(3):497-510.

48. Pei J, Grishin NV. Type II CAAX prenyl endopeptidases belong to a novel superfamily of putative membrane-bound metalloproteases. Trends Biochem Sci. 2001 May;26(5):275-7.

49. Pei J, Mitchell DA, Dixon JE, Grishin NV. Expansion of type II CAAX proteases reveals evolutionary origin of gamma-secretase subunit APH-1. J Mol Biol. 2011 Jul 1;410(1):18-26.

50. Howell-Adams B, Seifert HS. Molecular models accounting for the gene conversion reactions mediating gonococcal pilin antigenic variation. Mol Microbiol. 2000 Sep;37(5):1146-58.

51. Boles BR, Thoendel M, Roth AJ, Horswill AR. Identification of genes involved in polysaccharide-independent *Staphylococcus aureus* biofilm formation. PLoS One. 2010 Apr 14;5(4):e10146.

52. Fairweather N, Kennedy S, Foster TJ, Kehoe M, Dougan G. Expression of a cloned *Staphylococcus aureus* alpha-hemolysin determinant in *Bacillus subtilis* and *Staphylococcus aureus*. Infect Immun. 1983 Sep;41(3):1112-7.

53. Chen J, Yoong P, Ram G, Torres VJ, Novick RP. Single-copy vectors for integration at the SaPI1 attachment site for *Staphylococcus aureus*. Plasmid. 2014 Sep 2;76C:1-7.

54. Yarwood JM, Bartels DJ, Volper EM, Greenberg EP. Quorum sensing in *Staphylococcus aureus* biofilms. J Bacteriol. 2004 Mar;186(6):1838-50.

55. Monk IR, Shah IM, Xu M, Tan MW, Foster TJ. Transforming the untransformable: application of direct transformation to manipulate genetically *Staphylococcus aureus* and *Staphylococcus epidermidis*. MBio. 2012 Mar 20;3(2):10.1128/mBio.00277,11. Print 2012.

56. Bubeck Wardenburg J, Williams WA, Missiakas D. Host defenses against *Staphylococcus aureus* infection require recognition of bacterial lipoproteins. Proc Natl Acad Sci U S A. 2006 Sep 12;103(37):13831-6.

57. Alonzo F,3rd, Benson MA, Chen J, Novick RP, Shopsin B, Torres VJ. *Staphylococcus aureus* leucocidin ED contributes to systemic infection by targeting neutrophils and promoting bacterial growth in vivo. Mol Microbiol. 2012 Jan;83(2):423-35.

58. Thoendel M, Horswill AR. Identification of *Staphylococcus aureus* AgrD residues required for autoinducing peptide biosynthesis. J Biol Chem. 2009 Aug 14;284(33):21828-38.

59. Schagger H. Tricine-SDS-PAGE. Nat Protoc. 2006;1(1):16-22.

60. Lorenz U, Ohlsen K, Karch H, Hecker M, Thiede A, Hacker J. Human antibody response during sepsis against targets expressed by methicillin resistant *Staphylococcus aureus*. FEMS Immunol Med Microbiol. 2000 Oct;29(2):145-53.

61. Sakata N, Terakubo S, Mukai T. Subcellular location of the soluble lytic transglycosylase homologue in *Staphylococcus aureus*. Curr Microbiol. 2005 Jan;50(1):47-51.

62. Stapleton MR, Horsburgh MJ, Hayhurst EJ, Wright L, Jonsson IM, Tarkowski A, et al. Characterization of IsaA and SceD, two putative lytic transglycosylases of *Staphylococcus aureus*. J Bacteriol. 2007 Oct;189(20):7316-25.

63. Gray B, Hall P, Gresham H. Targeting agr- and agr-Like quorum sensing systems for development of common therapeutics to treat multiple gram-positive bacterial infections. Sensors (Basel). 2013 Apr 18;13(4):5130-66.

64. LaSarre B, Federle MJ. Exploiting quorum sensing to confuse bacterial pathogens. Microbiol Mol Biol Rev. 2013 Mar;77(1):73-111.

65. Park J, Jagasia R, Kaufmann GF, Mathison JC, Ruiz DI, Moss JA, et al. Infection control by antibody disruption of bacterial quorum sensing signaling. Chem Biol. 2007 Oct;14(10):1119-27.

66. Sully EK, Malachowa N, Elmore BO, Alexander SM, Femling JK, Gray BM, et al. Selective chemical inhibition of agr quorum sensing in *Staphylococcus aureus* promotes host defense with minimal impact on resistance. PLoS Pathog. 2014 Jun 12;10(6):e1004174.

67. Lyon GJ, Mayville P, Muir TW, Novick RP. Rational design of a global inhibitor of the virulence response in *Staphylococcus aureus*, based in part on localization of the site of inhibition to the receptor-histidine kinase, AgrC. Proc Natl Acad Sci U S A. 2000 Nov 21;97(24):13330-5.

VITA

Chelsea Rose White was born in Highland Park, IL on February 22, 1991 to Robert and Sherry White. She attended Mount Holyoke College, in Massachusetts where she received her Bachelor of Arts in Biology and Dance in May 2013. In 2014, Chelsea joined the Infectious Diseases and Immunology Research Institute's graduate program at Loyola University Chicago. After rotating through a few laboratories, Chelsea began to work under the mentorship of Dr. Francis Alonzo III, whose lab focuses on bacterial pathogenesis of *Staphylococcus aureus*. Chelsea's thesis has been focused on determining the role of a putative peptidase in facilitating quorum sensing and pathogenesis. Her time in the Alonzo lab has prepared her to accept a position as a Research Associate in Dr. Carrithers' lab at University of Illinois at Chicago where she will continue to develop as a scientist.

THESIS APPROVAL SHEET

The thesis submitted by Chelsea R. White has been read and approved by the following committee:

Francis Alonzo III, Ph.D., Director
Professor of Microbiology and Immunology
Loyola University Chicago

Karen Visick, Ph.D.
Professor of Microbiology and Immunology
Loyola University Chicago

James Cook, M.D.
Professor of Infectious Diseases
Loyola University Chicago

Katherine Radek, Ph.D.
Professor of Surgery
Loyola University Chicago

The final copies have been examined by the director of the thesis and the signature that appears below verifies the fact that any necessary changes have been incorporated and that the thesis is now given final approval by the committee with reference to content and form.

The thesis is therefore accepted in partial fulfillment of the requirements for the degree of Master of Science.

_____ _____

Date Director's Signature